

**GEOLOGY OF THE HENTY FAULT WEDGE,
WESTERN TASMANIA**

by

ROGER ANTHONY POLTOCK B.Sc.

Submitted in fulfilment of the requirements for the
degree of Master of Economic Geology

UNIVERSITY OF TASMANIA - DECEMBER 1992

This thesis contains no material which has been accepted for the award of any other higher degree or graduate diploma in any tertiary institution and, to the best of my knowledge and belief, the thesis contains no material previously published or written by another person, except when due reference is made in the text of the thesis.

Signed: 

ABSTRACT

The Henty Fault Wedge is a misfit slice of Cambrian lithologies which have been fault emplaced into the middle to late Cambrian Mt Read Volcanics. The Henty Fault Wedge has an exposed area of 30km² and is located midway between Queenstown and Rosebery in western Tasmania (Fig 1).

Two and possibly three fault juxtaposed structural domains occur within the wedge. The combined domains comprise six lithological associations, two tholeiitic volcanic/intrusive suites (Henty Valley and Ewart Creek Track Sequences), three calc-alkaline suites (Henty Adits, Halls Rivulet Track and Quartz phyrlic rhyolites) and an ophiolite complex. Igneous rocks are predominantly basaltic to andesitic in composition.

Metamorphic grade within the fault wedge is predominantly prehnite pumpellyite facies, with greenschist facies rocks only recognized in gabbros in the ophiolite complex.

Lithological and geochemical equivalents of the Henty Fault Wedge associations in western Tasmania are investigated. It is concluded that correlates of the Crimson Creek Formation and Mt Read Volcanics exist. The ophiolite complex is LREE and Zr enriched compared to other Tasmanian ultramafics; and andesites and tonalites within the complex have calc-alkaline affinities.

The South Henty Fault is the bounding structure to the wedge in the south east, and is interpreted to be the southern continuation of the Henty Fault, a major structure in western Tasmania.

The bounding structure to the west is the North Henty Fault, a Devonian structure which is interpreted to combine with the Rosebery Fault forming a north plunging thrust sole to a positive flower or pop up structure.

TABLE OF CONTENTS

| | PAGE |
|-------------------------------------------------------------------------------------------------------------------|------|
| LIST OF FIGURES | |
| LIST OF PLATES | |
| LIST OF TABLES | |
| LIST OF APPENDICES | |
| LIST OF ABBREVIATIONS | |
| ACKNOWLEDGEMENTS | |
| 1. INTRODUCTION | 1 |
| 2. REGIONAL GEOLOGY | 5 |
| 3. METHOD GEOCHEMISTRY - PETROLOGY | 8 |
| 4. ELEMENT MOBILITY AND SELECTION OF ELEMENTS AND PLOTS FOR DISCRIMINATION BETWEEN IGNEOUS LITHOLOGIES | 11 |
| 5. LITHOFACIES | 12 |
| 5.1 Introduction | 12 |
| 5.2 Henty Valley Sequence | 12 |
| 5.2.1 Introduction | 12 |
| 5.2.2 Quartz muscovite sandstone and siltstone | 13 |
| 5.2.3 Cherts | 16 |
| 5.2.4 Basaltic andesite | 18 |
| 5.2.5 Hematitic conglomerate greywacke and siltstone | 19 |
| 5.3 Henty Adits Sequence | 27 |
| 5.3.1 Introduction | 27 |
| 5.3.2 Sedimentary rocks | 27 |
| 5.3.3 Volcanics | 28 |
| 5.4 Halls Rivulet Track Sequence | 30 |
| 5.4.1 Introduction | 30 |

TABLE OF CONTENTS (cont.)

| | PAGE |
|---------------------------------------------------------------|-------------|
| 5.4.2 Sedimentary rocks | 30 |
| 5.4.3 Volcanics | 31 |
| 5.5 Ophiolite complex | 32 |
| 5.5.1 Introduction | 32 |
| 5.5.2 Sedimentary rocks | 33 |
| 5.5.3 Volcanics | 34 |
| 5.5.4 Intrusives | 35 |
| 5.5.5 Cumulates | 36 |
| 5.5.6 Geochemistry of the ophiolite | 37 |
| 5.6 Ewart Creek Track Sequence | 39 |
| 5.6.1 Introduction | 39 |
| 5.6.2 Sedimentary rocks | 39 |
| 5.6.3 Volcanics and intrusives | 40 |
| 5.7 Quartz-phyric rhyolite | 42 |
| 5.8 Lithofacies Summary | 43 |
| 6. LITHOLOGICAL AND GEOCHEMICAL EQUIVALENTS OF | |
| HENTY FAULT WEDGE UNITS IN WESTERN TASMANIA | 45 |
| 6.1 Definition of regional Cambrian units in Western Tasmania | 45 |
| Crimson Creek Formation | |
| Ultramafics | |
| Western Volcanosedimentary Sequence | |
| Central Volcanic Complex | |
| Tyndall Group | |
| 6.2 Previous correlation of units | |
| within the Henty Fault Wedge | 47 |

TABLE OF CONTENTS (cont.)

| | PAGE |
|-----------------------------------------------------------|-------------|
| 6.3 Correlation of sequences in the Henty Fault Wedge | 48 |
| 6.3.1 Henty Valley Sequence | 48 |
| 6.3.2 Henty Adits Sequence | 50 |
| 6.3.3 Halls Rivulet Track and Ewart Creek Track Sequences | 54 |
| 6.3.4 Ophiolite | 56 |
| 7. TECTONIC SETTING OF VOLCANICS AND INTRUSIVES | 60 |
| 7.1 Henty Valley Sequence | 60 |
| 7.2 Henty Adits - Halls Rivulet Track basaltic andesite | 60 |
| 7.3 Ewart Creek Sequence | 61 |
| 7.4 Ophiolite | 61 |
| 8. STRUCTURAL GEOLOGY | 63 |
| 8.1 Introduction | 63 |
| 8.2 South Henty Fault | 64 |
| 8.3 North Henty Fault | 65 |
| 8.4 Howards Tramway Fault | 66 |
| 8.5 Relationships between faults/fault movements | 66 |
| 9. CONCLUSIONS | 69 |
| REFERENCES | 71 |

LIST OF FIGURES

1. Geologic map of western Tasmania showing the distribution of the major volcano-sedimentary units and the locations of major VHMS deposits (from Stolz & Large 1992).
2. Interpretive Geology EL 11/85 Henty Area 1: 25000
3. Enhanced aeromagnetics EL 11/85 Henty Area, colour drape, sun angle 305° @ 70° and interpretive geology overlay. 1: 50000
4. Stratigraphic section - Eastern Henty Fault Wedge.
5. Plot of analysis of chrome spinel grains from Henty Fault Wedge ultramafics and greywackes. Plus fields of chrome spinel analysis from Cambrian mafic - ultramafic lavas and cumulates from the Dundas Trough.
6. Ti-Zr plot, showing fields for Henty Fault Wedge lavas and intrusives.
7. Na₂O + K₂O - FeO - MgO plot, differentiation of tholeiite and calc-alkaline series lavas and intrusives from the Henty Fault Wedge. Fields of tholeiite (TH) and calc-alkaline (CA) compositions after Irvine and Baragar, 1971.
8. Ti/Zr-SiO₂ (mass %) plot for Henty Fault Wedge lavas and intrusives.
9. Chondrite-normalized REE patterns for Henty Fault Wedge igneous rocks.

| | |
|------------------------------------|---------------------------------|
| a) Henty Valley basaltic andesites | CLbn ₃ |
| b) Henty Adits basaltic andesites | CLbn ₂ |
| c) Halls Rivulet Track andesite | CLbn ₁ |
| d) Ewart Creek basalt | CL/Ib |
| e) Ophiolite complex | Cus Cg Clg Clt CVn ₁ |
| f) Rhyolites | CVr |
10. PRIM-normalized geochemical patterns for Henty Fault Wedge igneous rocks.

| | |
|-----------------------------------|---------------------------------|
| a) Henty Valley basaltic andesite | CLbn ₃ |
| b) Henty Adits basaltic andesite | CLbn ₂ |
| c) Halls Rivulet Track andesite | CLbn ₁ |
| d) Ewart Creek basalt | CL/Ib |
| e) Ophiolite complex | Cus Cg Clg Clt CVn ₁ |
| f) Rhyolite | CVr |

11. Stratigraphic section - Western Henty Fault Wedge.
12. Stratigraphic and structural relationships between the Ewart Creek/Truscott Creek Sequences - Yolande River Sequence - Ordovician Denison Group. Based on HFW mapping, Tas. Dept. Mines Strahan and Queenstown 1:5000 Series and MRV Map 3.
13. Comparison of chondrite normalized REE plots for Henty Valley tholeiites and Crimson Creek Formation tholeiites (from Brown 1986).
14. Ti/Zr - SiO₂ (mass %) plot, comparison of HFW igneous suites with Mt Read Volcanic Suites I-V from Crawford et al 1992 (fields for Suites I-V are shown).
15. Zr-SiO₂ (mass %) plot, a comparison of two mafic-ultramafic associations in western Tasmania. Data is from the HFW (Table 2), from McClenaghan and Findlay 1989 (Table 4) and from Olubas 1989.
16. A comparison of chondrite-normalized REE patterns for mafic-ultramafic complexes in western Tasmania. For data sources and rock types see Table 4.
 - a) Henty Fault Wedge
 - b) Timbertops
 - c) McIvor Hill and Macquarie
17. Domain map of the Zeehan - Lake Selina region (from Keele 1991).
18. Interpretive structural sections 1:100000
 - a) 5367000N Mt Hamilton - Mt Read - Anthony Dam,
modified from Keele (1991).
 - b) 5358500N Mt Dundas - Newton Creek Dam - Sticht Range, compiled
from HFW mapping and Corbett MRV Map 3. Geol. Surv. Tas.

LIST OF PLATES

1. View west from the Tyndall Range across the Henty Fault Wedge
2. 31666 Henty Valley tholeiitic vesicular basalt - sericite/pyrite altered (plane polarized light).
3. 31683 Henty Valley tholeiitic basalt lava or sill (crossed nicols).
4. 30136 Henty Valley hematitic wacke - opaque hematite cement - chrome spinel grain centre of view (plane polarized light).
5. 30862 Henty Adits basaltic andesite - flow orientated plagioclase phenocrysts (plane polarized light).
6. 30141 Halls Rivulet Track volcanoclastic sandstone - angular quartz crystal fragments - zircon grains - quartz sericite matrix (crossed nicols).
7. 30024B Halls Rivulet Track andesite-plagioclase and augite phyric (plane polarized light).
8. 30103B Ophiolite Complex andesite lava - quenched pyroxene (plane polarized light).
9. 30155 Ophiolite Complex - chilled contact between dolerite and andesitic dyke-actinolite development in dolerite pyroxenes (crossed nicols).
10. 30085 Ophiolite Complex tonalite intrusive - poikiloblastic quartz (crossed nicols).
11. Dacite - rhyolite quartz porphyries (plane polarized light)
 - a) 32170 from the White Spur Creek Fault within the HFW
 - b) 30099 from within the South Henty Fault at 53000N
 - c) 30072 Yolande River Sequence adjacent to the SHF

LIST OF TABLES

1. Comparison of Henty Valley Cherts with Cretaceous biogenic and hydrothermal cherts.
2. Major element analysis of Henty Valley greywackes from DDH HR3.
3. Symbols used on geochemical plots for Henty Fault Wedge rocks.
4. Geochemical differences between Henty Adit Sequence basaltic andesite and Que Hellyer footwall andesites.
5. Rock descriptions and analytical data sources for samples plotted in Fig 16b and c.

LIST OF APPENDICES

1. Henty Fault Wedge sample catalogue.
2. Major, trace and rare earth element analysis for Henty Fault Wedge igneous rocks.
3. Major element analysis for Henty Valley cherts and greywackes.
4. Chemical analysis and structural formulae of chrome spinels from ultramafics (30091), quartz muscovite sandstone (32153) and hematite facies greywacke (30989).

LIST OF ABBREVIATIONS

| | |
|------|-----------------------------------------------------------------------|
| ACG | Animal Creek Greywacke |
| AI | Alteration index $AI = 100 (K_2O + MgO) / (K_2O + MgO + Na_2O + CaO)$ |
| CCF | Crimson Creek Formation |
| Cr# | $(100 \times Cr) / (Cr + Al)$ |
| CVC | Central Volcanic Complex |
| ECTS | Ewart Creek Track Sequence |
| EL | Exploration Licence |
| HAS | Henty Adits Sequence |
| HF | Henty Fault |
| HFW | Henty Fault Wedge |
| HRTS | Halls Rivulet Track Sequence |
| HVS | Henty Valley Sequence |
| Mg# | $(100 \times Mg) / (Mg + Fe)$ |
| Mg* | $Mg / (Mg + Fe)$ |
| MRS | Miners Ridge Sandstone |
| MRV | Mt Read Volcanics |
| NHF | North Henty Fault |
| SHF | South Henty Fault |
| WSCF | White Spur Creek Fault |
| WVSS | Western Volcano Sedimentary Sequence |
| YRS | Yolande River Sequence |

ACKNOWLEDGEMENTS

I would like to thank Pasminco Exploration for making the study area and analytical data available; in particular Fergus FitzGerald for his support during the project and Gillian Bennett for her drafting skills. I would also like to thank the following people: Jocelyn McPhie and Joe Stolz my supervisors, for their help during the course and constructive criticism of the draft manuscript. Ross Large, the CODES staff and course participants for their support and enthusiasm during the Master of Economic Geology course. Tony Crawford for his discussions on petrological and geochemical matters. Phillip Robinson for analytical work and provision of analytical standards. Wieslaw Jablonski for his patience and guidance in the use of the electron microprobe. Meg Taylor and Christine Stocks for proof reading the draft manuscripts.

1. INTRODUCTION

The study area of 30km² covers virtually the entire Henty Fault Wedge (HFW). The wedge is bounded by the North and South Henty Faults and consists of folded and faulted Cambrian sedimentary, volcanic and intrusive rocks. The Cambrian age is constrained by a single fossil locality (Corbett and Lees 1987).

The HFW lies within Pasminco's Exploration Licence 11/85; and is located midway between Queenstown and Rosebery in western Tasmania (Fig 1). The area is accessed by the Zeehan Highway in the south, and Howards and Anthony Roads in the west and east respectively (Fig 2). Vehicular access within the HFW is limited to the Halls Rivulet Track; beyond this, access is via a system of east - west gridlines established by Pasminco Exploration.

Topography is steep, the main feature being the Henty River valley (Plate 1) which flows along the South Henty Fault (SHF), the bounding structure to the east. Vegetation is dense temperate rainforest which frequently has an impenetrable understory.

Rock exposure is poor. Mapping is based on isolated outcrops; float and soil type changes along grid lines, with additional detail from stream traverses. Most soils are residual but Quaternary fluvio-glacials obscure outcrop on the plateau at 500mASL and in the lower sections of the Henty River valley.

Drilling has only been carried out at the Henty Adits Prospect in the central eastern area (Meares, 1980) and in vicinity of the Zeehan Highway (Corbett, 1985).

The aims of this study are to define:

- lithostratigraphic units within the HFW and correlate these with other sequences in western Tasmania, with the emphasis being placed on the prospective Mt Read Volcanics (MRV).
- tectonic settings implied by the composition and lithological associations of igneous units.
- structures within and bounding the fault wedge and establish their relationship to regional structures.

The study has been carried out in conjunction with exploration for volcanic hosted massive sulfide mineralization by Cyprus Gold and Pasminco Exploration, and has entailed geological mapping, petrology, lithogeochemistry, electron microprobe analysis of detrital mineral grains and aeromagnetics interpretation.

Previous work on the HFW has been principally exploration geology on EL 9/66 by the Mt. Lyell Co. and Getty Oil Development Co., and EL 11/85 by Cyprus Gold, EZ Co. and Pasminco Mining and Exploration. The most detailed study has been completed by Meares (1980) on the setting of the Henty Adits mineralization. Exploration has been primarily directed toward locating volcanic hosted base and precious metal mineralization; methods used by the companies included geochemistry, geophysics, diamond drilling and prospect scale mapping. As a result of this exploration the Henty Prospect gold mineralization has been located by Renison Goldfields within the Henty Fault zone approximately 1km north of the HFW apex.

The HFW has been included in regional surveys by the Tasmanian Department of Mines and work includes:

- Corbett and Lees (1987), recognizing the HFW as a "misfit sequence" within the Mt Read Volcanic Central Volcanic Complex.
- Corbett and McClenaghan (1985), a regional survey of the geochemistry of MRV, defining tholeiitic basalts in the western sector of the wedge and calc-alkaline andesites in the central area.

Subdivision of the MRV on the basis of geochemistry and lithological associations by Crawford et al (1992) has included the calc-alkaline volcanics and the Ewart Creek Track Sequence tholeiites with their Suites I and IV respectively.

Newton Spillway

Mt. Dundas

Henty Gold Prospect

Mt. Read

Mt. Murchison



PLATE I

View west across the Tyndall, Henty Fault Wedge and White Spur areas

E.L. 11/85

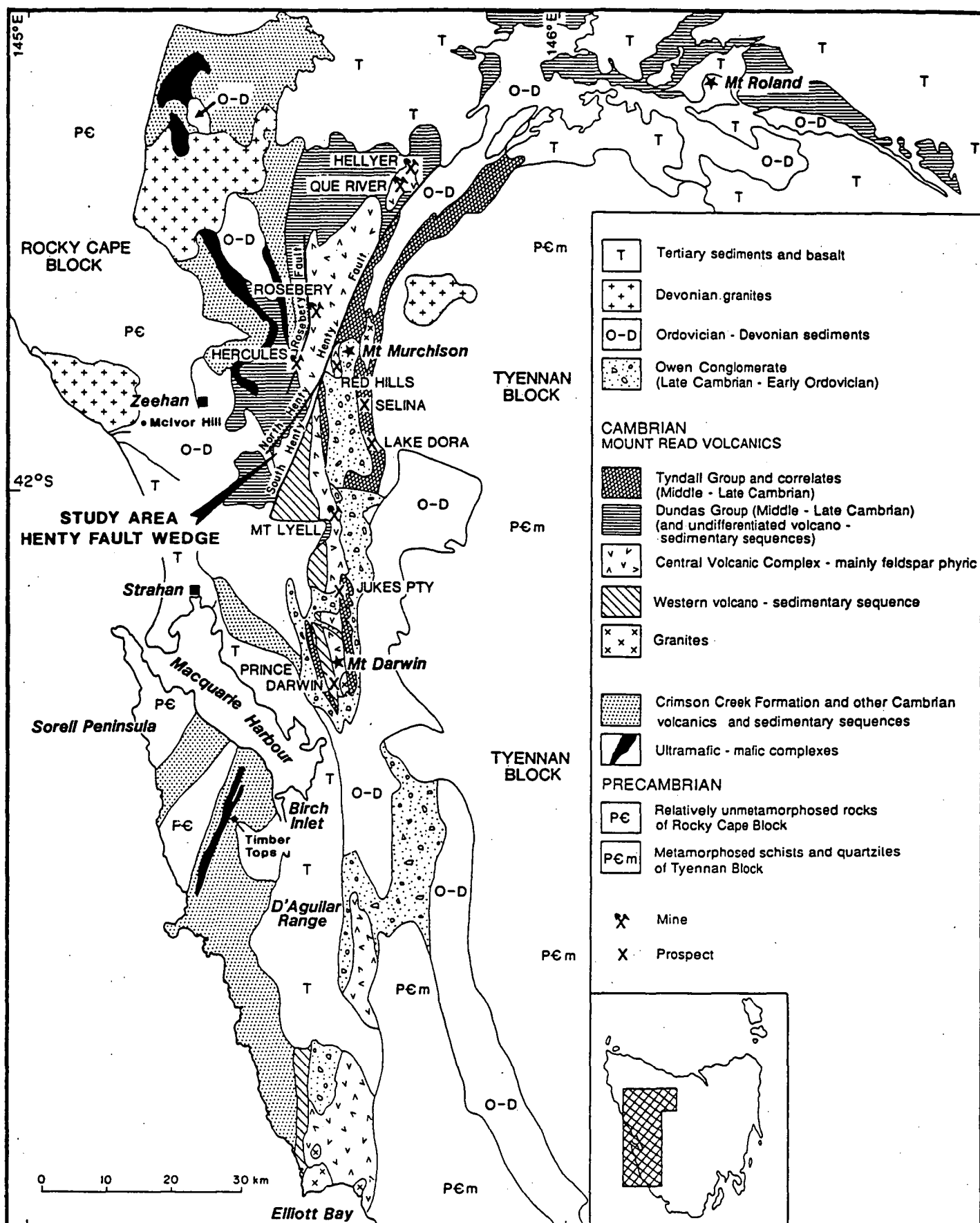


FIGURE 1

GEOLOGIC MAP OF WESTERN TASMANIA SHOWING THE DISTRIBUTION OF THE MAJOR VOLCANO-SEDIMENTARY UNITS AND THE LOCATIONS OF THE MAJOR VHMS DEPOSITS

(from STOLZ and LARGE, 1992)

2. REGIONAL GEOLOGY

Basement in western Tasmania is the Proterozoic which comprises siltstone, turbidites, dolomite, basalts and dolerites. These rocks are dominantly green-schist facies assemblages with higher grade amphibolite and eclogite facies relics (Turner, 1989); this metamorphism and deformation predates Cambrian deposition. The basement is exposed east of the study area as the Tyennan Block and to the north west as the Rocky Cape Block (Fig 1).

Cambrian volcanism and sedimentation developed on this continental crust, and can be subdivided into the eo-Cambrian tholeiitic Crimson Creek Formation (CCF) and the mid to late Cambrian predominantly calc-alkaline Mt Read Volcanics (MRV).

The eo-Cambrian CCF tholeiitic basalts and sedimentary rocks were deposited in shallow but rapidly subsiding basins (Brown, 1986 and Haines, 1991) which developed on an attenuated rifted passive continental margin (Crawford and Berry, 1991). Sedimentary rocks include hematite facies turbidites, basaltic volcanoclastics, carbonates, evaporites and cherts (Brown, 1986 and Haines, 1991). The CCF occurs in the Dundas, Smithton and Dial Range Troughs.

Ultramafic cumulates and volcanic equivalents were thrust onto the CCF in the mid Cambrian. The occurrence of boninite lavas with ultramafics indicates formation in the fore-arc of an oceanic island arc setting (Crawford and Berry, 1991).

The MRV form a 200km long by 20km wide north south trending belt along the eastern side of the Dundas Trough, adjacent to and in some areas onlapping and intruding the Precambrian basement. The volcanics include intermediate

to felsic lavas, subvolcanic porphyries and granites, volcanoclastics and basement derived sedimentary rocks.

Corbett and Lees (1987) subdivided the MRV into four lithostratigraphic subdivisions; Central Volcanic Complex (CVC), Western Volcanosedimentary Sequence (WVSS), Dundas Group (DG) and Tyndall Group (TG).

The volcanics have also been subdivided on the basis of geochemistry into three calcalkaline and one tholeiitic suite (Crawford et al, 1992). These geochemical subdivisions to a large extent compliment those based on lithostratigraphy made by Corbett and Lees (1987).

The MRV host five economically significant volcanic hosted massive sulfide deposits (Fig 1). Two styles of mineralization occur, stratabound massive Pb Zn Cu Ag Au (Rosebery, Hercules, Hellyer and Que River) and disseminated Cu Ag Au (Mt Lyell).

The Henty Fault (HF) is a regional N to NNE trending, steep west dipping structure which cuts obliquely across the MRV. The fault has a complex history of movement which includes reverse, dip, slip and wrench components (Berry 1989). The structure was active during the Cambrian, early Ordovician and Devonian. Regional features associated with the fault include:

- MRV associated granitoids only occur SE of the fault.
- mineralization in the MRV is Pb Zn Cu Ag Au massive sulfide to the NW and predominantly Cu Ag Au disseminated sulfides to the SE of the fault.
- the fault has acted as a focus for late Cambrian Henty Dyke Swarm tholeiitic magmatism.

- control of Cambro-Ordovician depositional basins, thick Denison Group conglomerates occur SE of the fault.

Cambrian volcanism and sedimentation is followed by basal Ordovician siliciclastics of the Denison Group. These were derived mainly from Precambrian metamorphics with some volcanic detritus in the basal sections. The basal conglomerates are thick wedges controlled either by extensional rift basins adjacent to the Tyennan Block metamorphics or accumulations at the western edge of the Tyennan metamorphic thrust sheets (Berry, 1991). The Denison group rests unconformably on the Cambrian indicating some Cambrian deformation.

The Denison group is followed by the regionally transgressive Gordon Group marine carbonate and Siluro-Devonian Eldon Group sandstone and shale.

At least two phases of regional compression, D1 east west and D2 north south (Keele, 1991), were associated with the mid Devonian Tabberabberan Orogeny. The development of folding, cleavage and regional thrusts in lower Palaeozoic rocks was associated with this event.

Tabberabberan deformation is followed by extensive intrusion of Devonian to Carboniferous granitoids which have characteristics associated with both I and S type granites (McClenaghan, 1989). These granites are associated with carbonate replacement tin mineralization at Renison Bell and Mt. Bischoff, and the Pb Zn Ag vein deposits of the Zeehan field.

MAGNETICS - COLOUR DRAPE

SUN 305° 70°

E.L. 11/85
HENTY AREA

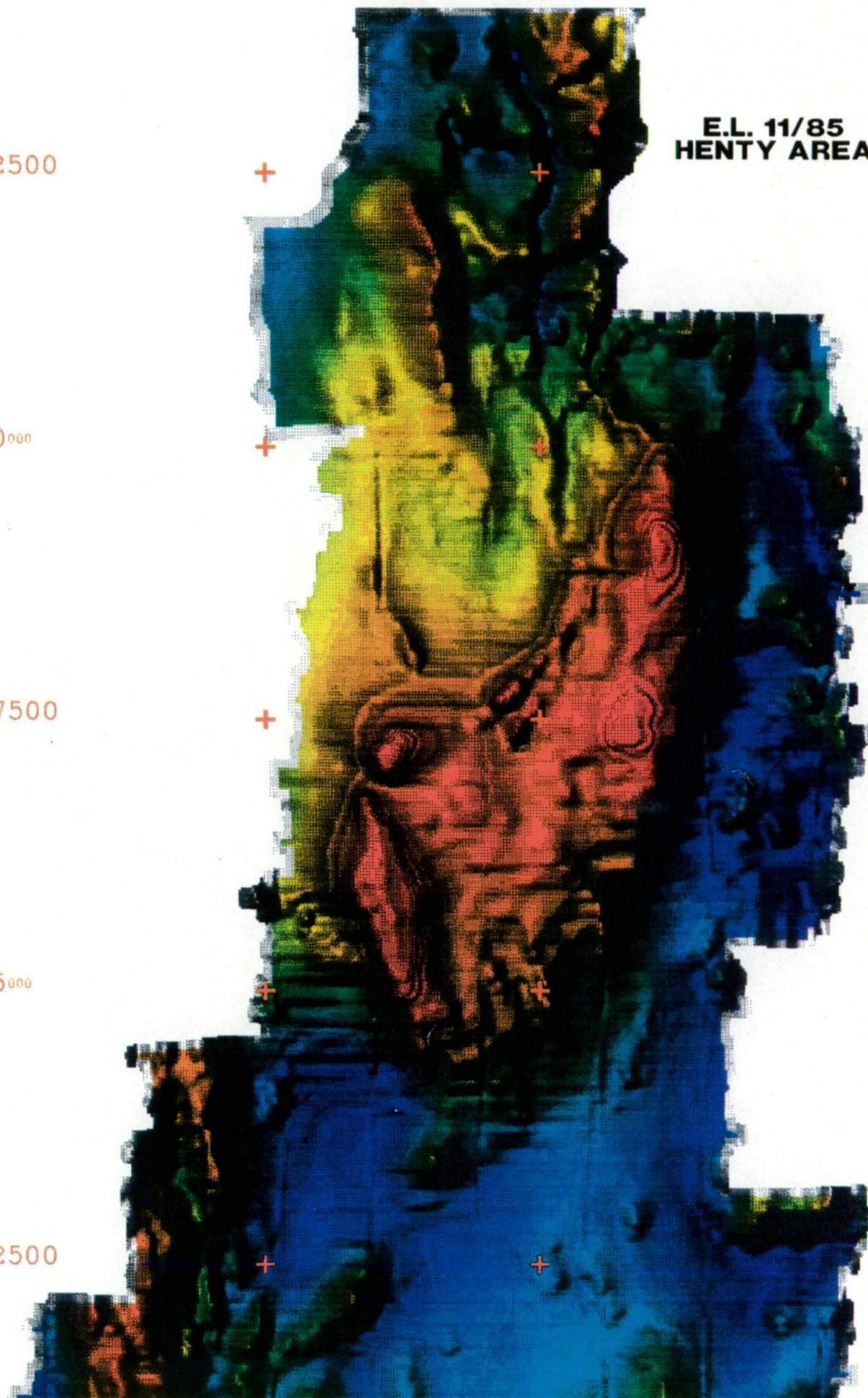
5362500

5360000

5357500

5355000

5352500



3. METHODS GEOCHEMISTRY - PETROLOGY

Appendix 1 tabulates all rock samples used in the study, their coordinates and work undertaken.

A total of 30 rock samples of lavas and intrusives were selected from the six mapped units. The least altered rocks were selected for analysis on the basis of thin section examination, with the exception of pervasively altered units. These altered samples include No's 31641, 31666, 32170 (sericite chlorite pyrite) and No's 30124, 31676 (carbonate altered). The latter group had alteration indices (AI) between 75 and 94. This index $[AI = 100(K_2O + MgO)/(K_2O + MgO + Na_2O + CaO)]$ is a measure of the sericite chlorite alteration of feldspars (Date et al., 1983).

Rocks were crushed to -20mm in a tungsten carbide faced crusher at Analabs Laboratory, Burnie. Approximately 200gm of coarse crushed material was hand-picked avoiding alteration, veins, weathered surfaces, and powdered in a tungsten carbide ring mill.

Analysis of major and trace elements were carried out at the Geology Department University of Tasmania by Phillip Robinson using X-ray fluorescence spectrometry on fused beads and pressed powders, according to the method described by Norrish and Chappell (1967).

Major element analysis were recalculated 100% volatile-free to facilitate comparison of samples with variable modal amounts of hydrous minerals eg chlorite and calcite formed during alteration and metamorphism. The maximum loss on ignition was 11.48% in carbonate altered sample No 30124. Analysis are listed in Appendix 2.

Three duplicates, No's 30085, 30155 and 30857 were analyzed to establish within sample variations and two Geology Department University of Tasmania standards each of TASBAS, TASGRAN and TASMONTZ were included to check analytical variations. No significant variations were registered in duplicates or standards.

On the basis of mapped units and major/trace element lithogeochemical groups, a representative suite of 13 samples were analyzed for REE by Becquerel Laboratories by method GN805 (extended counting time). Analysis are listed in Appendix 2.

Chert and hematitic greywacke samples were analyzed at Analabs by method OX 408 - XRF (major elements) and method GX 401 - XRF (Rb Sr Y Zr). This data is listed in Appendix 3.

Other data sources include:

- sample No. 12B McIvor Hill (Crawford, pers com, 1992).
- sample No. 81735 Henty Fault Wedge (Jenkins, 1990).
- sample No's 41516, 41543 and MH 565 Macquarie (McClenaghan and Findlay, 1989).

Chrome spinel grains in sedimentary rock samples No's 30989 and 32153, and ultramafic sample No. 30091 were probed using the Cameca SX50 microanalytical system at the Central Science Laboratory, University of Tasmania. Data is listed in Appendix 4.

A total of 82 thin sections of igneous and sedimentary lithologies were examined.

Of these, 32 were described by Tony Crawford and two by Stan Joyce (Geochempet Services) for Pasminco Exploration and Cyprus Gold in the course of exploration on EL 11/85. These petrological reports are included as appendices in EL 11/85 annual reports (see Poltock and FitzGerald, 1991 and Poltock, 1992).

4. ELEMENT MOBILITY AND SELECTION OF ELEMENTS AND PLOTS FOR DISCRIMINATION BETWEEN IGNEOUS LITHOLOGIES

It has been established by Pearce and Cann (1973) that elements are mobile to varying degrees during alteration and metamorphism and hence analysis of ancient volcanic rocks may not reflect abundances in the original magma.

The most mobile elements are:

- MgO K₂O Na₂O CaO FeO, the mobility of these oxides is well documented and has been used in defining alteration zones in volcanogenic massive sulfide systems (Green, 1990).
- SiO₂, in relatively unaltered rocks SiO₂ should be within 1-3% of primary abundances (Crawford et al, 1992).
- Ba Sr are particularly sensitive to alteration and weathering (Pearce and Cann, 1973).

The least mobile elements include Ti Zr Y Nb Cr and REE. The relative immobility of these elements has been documented by Floyd and Winchester (1975), and Pearce and Cann (1973). However a degree of mobility is suggested by Finlow-Bates and Stumpfl (1981) for REE, Y and Nb in altered andesites and dacites at Que River. Alteration of the Que River volcanics is more intense than in the HFW samples.

The least mobile elements have been used to determine primary geochemical affinities of igneous rock suites, define differentiation trends in these suites and to assign igneous suites to palaeo-tectonic settings.

5. LITHOFACIES

5.1 INTRODUCTION

Subdivision of the HFW sequence is based primarily on mapped lithological associations, petrology and lithogeochemistry with support from aeromagnetism (Fig 3). Six sequences have been recognized within the HFW and include the Henty Valley, Henty Adits, Halls Rivulet Track, Ophiolite complex, Ewart Creek and rhyolites (Fig 2). The sequences will be discussed from the interpreted stratigraphic base to top (Figs 4 and 11).

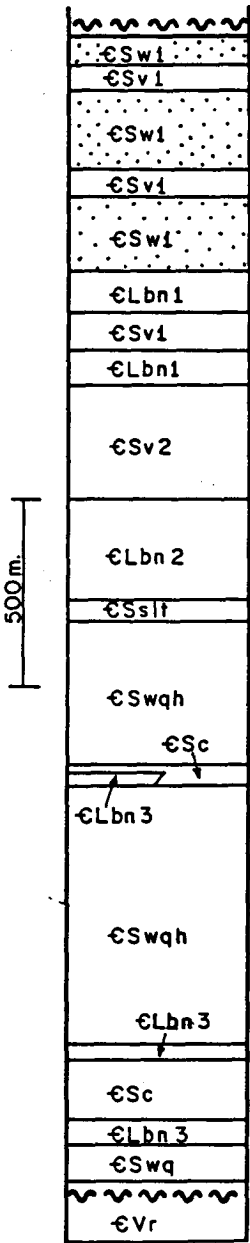
Volcanic suites are subdivided into calc-alkaline and tholeiitic using the alkali-FeO-MgO plot (Fig 7); further subdivision is based on SiO₂ content and follows that defined by BVSP (1981), <53% basalt, 53-57% basaltic andesite, 58-63% andesite, 64-68% dacite and >68% rhyolite.

5.2 HENTY VALLEY SEQUENCE CSwq CSc CLbn3 CSwqh

5.2.1 Introduction

The Henty Valley Sequence (HVS) consists of quartz sandstone, chert, hematitic wacke/siltstone and basaltic andesite. The most extensive exposures are in Halls Rivulet and at the Henty Valley Prospect (Fig 2). The two occurrences are displaced by a dextral strike slip movement on a splay of the SHF.

From graded bedding the sequence faces west; the oldest sedimentary units exposed occurring within the SHF, hence the relationship to underlying geology is unknown (Fig 4). The upper limit is well defined by drilling at the Henty



FAULT

CAMBRIAN

HALLS RIVULET TRACK SEQUENCE

TYNDALL GROUP or YOLANDE RIVER SEQUENCE



Henty Adits Basaltic Andesite and Transition Sequence

HENTY VALLEY SEQUENCE

YOLANDE RIVER SEQUENCE or CRIMSON CREEK FORMATION

SOUTH HENTY FAULT

Refer to 1:25000 Legend

| | | |
|----------------------------------------------------------------------------------------------------------------------------------------------------------------------------|---------------------------------------------------------------------------------------------|---------------|
|  PASMINCO EXPLORATION <small>A Division of Pasminco Australia Limited</small> | | |
| COMPILED: R.A.P. | STRATIGRAPHIC SECTION EASTERN HENTY FAULT WEDGE | |
| DATE: 27-6-'92 | | |
| DRAWN: N.W.D.S. | | |
| REF.: | | |
| REVISIONS: | | |
| DRAWING No. | SCALE  | FIG. No. 4 |

Adits Prospect where siltstone and andesitic volcanics of the Henty Adits Sequence overlie it with apparent conformity (Meares, 1980).

5.2.2 Quartz muscovite sandstone and siltstone CSwq

The sandstone and siltstone are exposed in the Henty River at the confluence with Newton Creek and at Henty Valley. Sheared and carbonate altered sandstone within the SHF which were intersected in DDH BR1 between 445.7-502.0m (Corbett, 1985) are interpreted to belong to the same sequence.

At Newton Creek the sandstone occurs in open folds and is thickly bedded with grey to black siltstone partings, representing graded units 0.5-0.75m thick. At Henty Valley, the sequence is dominated by graphitic and pyritic siltstone with subordinate sandstone, limestone and massive pyrite. The latter occurs as laminae to 1m thick beds.

Sandstone is moderately well sorted, fine to coarse grained and composed of detrital grains 0.1-1.0mm that include polycrystalline quartz, tourmaline, chrome spinel and muscovite.

Lithics are 1-4mm and include siltstone, quartzite, chert and quartz muscovite schist. The detritus has been derived almost entirely from a pelitic and psammitic metasedimentary terrane of probable Precambrian age, with subordinate input from chrome spinel bearing Cambrian ultramafics. Chrome spinel grains were probed and Cr# [$\text{Cr\#} = 100\text{Cr}/(\text{Cr} + \text{Al})$] ranged from 86.56-92.20 (Appendix 4); the high Cr# in sample 32153 is indicative of derivation from boninite lavas and their comagmatic cumulates which occur in the Dundas Trough (Brown, 1986). Figure 5 shows Cr# versus Mg# [$\text{Mg\#} = 100\text{Mg}/(\text{Mg} + \text{Fe})$] for the chrome spinel grains from the sandstone and fields from

chrome spinels from Tasmanian mafics and ultramafics.

Relative maturity of the sandstone is indicated by grainsize sorting. The mixed metamorphic and ultramafic detritus is evidence of reworking and storage of detritus prior to deposition.

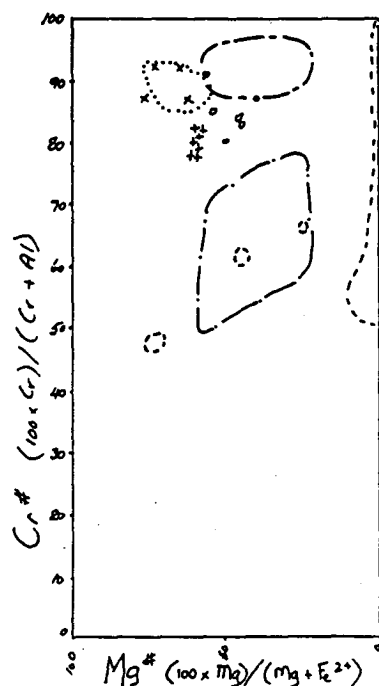


Fig.5 Plot of analysis of chrome spinel grains from Henty Fault Wedge ultramafics and greywackes. Plus fields of chrome spinel analysis from Cambrian mafic - ultramafic lavas and cumulates from the Dundas Trough.

Henty Fault Wedge

- + 30091 Cus
- x 32153 CSwq
- o 30989 CSwqh

Dundas Trough

- Boninites (Brown 1986)
- Layered dunite harzburgite (Brown 1986)
- Layered pyroxenite dunite (Brown 1986)
- Miners Ridge Basalt (Dower 1981)

5.2.3 Chert CSc

The most extensive exposures of chert are in the Henty River between 75150-75260E and waterfalls in the Henty River tributaries at 75150E, 50450N and 75400E, 51525N. Minor chert and chert pebble conglomerates occur in the Halls Rivulet area. The cherts are closely associated with basaltic andesite lavas in the basal section of the Henty Valley Sequence (Fig 4) and probably predate the hematitic conglomerate and greywacke, clasts of chert frequently occurring in the latter.

Cherts are massive to weakly bedded and occasionally brecciated. This brecciation may be an effect of burial diagenesis; it has been recognised by Greensmith (1989) that the diagenesis of chert may take up to 80my and late stages are particularly prone to brecciation.

In thin sections the cherts are very fine grained, and separate components are irresolvable. In some siliceous siltstones concentric structures <3mm were tentatively identified as oolites; two polished surfaces were scanned with an electron microscope but failed to locate any features suggestive of oolites or radiolaria.

The cherts have a compositional range in SiO₂ from siliceous siltstone 72% to chert 94% (Appendix 3). Colour ranges from white-grey-green-red; the latter is a siliceous laminated siltstone with 7.1% FeO.

Major and trace element geochemistry of these cherts has been compared with data on Cretaceous siliceous sediments from the North Pacific (Adachi et al, 1986). Adachi et al 1986 used geochemistry and textural evidence to differentiate between hydrothermal and biogenic cherts.

Hydrothermal cherts are characterized by abundance of quartz veins, fluid inclusions, high Fe_2O_3 and MnO content and contain minimal terrigenous material. These cherts have a restricted spatial distribution and are closely associated with mid ocean ridges and submarine basaltic volcanism.

Biogenic cherts containing lower levels of Fe_2O_3 and MnO, have a significant terrigenous component and abundant biogenic remains; these cherts are laterally more extensive and although frequently associated with basaltic volcanics are not considered to be of hydrothermal origin (Imoto, 1983 and Hesse, 1988). Geochemical features of the two chert types are summarised in Table 1. From this table it can be seen that HFW cherts have greater affinities with the biogenic cherts.

The Henty Valley cherts are interpreted to have precipitated from the tests of marine organisms in an oceanic environment with minimal terrigenous material being introduced. The association of cherts with ocean floor basalts is discussed by Imoto (1983) and Hesse (1988). Their conclusion is that the common link is not a hydrothermal system but that tectonic and oceanographic conditions associated with oceanic volcanism are the same conditions required for the generation of cherts.

Table 1. Comparison of Henty Valley cherts with Cretaceous hydrothermal and biogenic cherts from the North Pacific.

| | Leg 32 hydrothermal chert | Kamiaso biogenic chert | *HFW chert |
|--------------------------------------------------|------------------------------------------|---------------------------------------|-----------------------|
| Al/(Al+Fe+Mn) | 0.01 | 0.60 | 0.55 |
| Fe ₂ O ₃ | 2.53% | 0.98% | 1.30% |
| Al ₂ O ₃ /TiO ₂ | 10.40 | 19.90 | 19.70 |
| Fe ₂ O ₃ /TiO ₂ | 50.60 | 9.80 | 12.83 |
| MnO/TiO ₂ | 8.60 | 0.40 | 0.79 |

*HFW Henty Fault Wedge average value for samples 30175 and 32842

5.2.4 Basaltic andesite CLbn3

These lavas and possibly intrusives are of limited extent occurring at the Henty Valley Prospect, 5359600N in the Henty River and Halls Rivulet at 76850E. The bodies are between 10-20m thick and either in contact with or closely associated with cherts, and overlain by the hematitic greywacke conglomerate (Fig 4).

Lavas are aphyric to slightly plagioclase - phyric, massive to highly vesiculated to the extent that it is difficult to determine if they were monomict scoriaceous breccias or coherent lavas (Plate 2). Lavas are pervasively altered at Henty Valley, particularly the more vesiculated type. The alteration assemblage includes calcite, sericite, pyrite and hematite. The AI for sample No's 31641 and 31666 is 75.

Intrusives are almost aphyric with minor plagioclase phenocrysts in an ophitic groundmass of albitized plagioclase, augite and abundant FeTi oxides (Plate

3). Scattered carbonate - hematite amygdales occur in some intrusives.

Geochemically the basaltic andesites can be defined as tholeiites on Ti-Zr plot (Fig 6) and AFM plot (Fig 7). The basaltic andesites can be distinguished from other suites in the HFW on the Ti/Zr-SiO₂ plot (Fig 8). TiO₂ and Nb values are high compared to other suites and range from 2.13-3.84% for TiO₂ and 18-24ppm for Nb (Fig 10a). The REE plot (Fig 9a) is nearly flat with very slight LREE enrichment; the (La/Yb)/N ratios for the two samples are 2.7 and 3.0.

5.2.5 Hematitic conglomerate greywacke and siltstone CSwqh

These hematitic rocks form the largest proportion of the HFW and are exposed primarily to the north of Henty Adits and two small fault bound blocks at 53000N and Henty Valley (Fig 2). One of the better exposures of the conglomerate and greywacke is in the Henty River at 75150E and a tributary at 75150E 51000N. The nature of the basal contact is poorly defined but probably overlies the cherts and the Henty Valley Sequence basaltic andesites; the upper contact is transitional with the Henty Adits Sequence (Fig 4), and has been described by Meares (1980) in DDH HR1, 2, 3, at the Henty Adits Prospect.

The unit is mainly siltstone-greywacke with frequent conglomerate and occasional chert, dolomite and basaltic andesite lens. There has been no attempt to define the internal stratigraphy of this unit and some of the apparent thickness (+1000m) may be due to structural repetition (Leaman, 1991), Meares (1980) has defined 468m of true thickness in DDH HR 3 at Henty Adits.

The conglomerates are variably monomict to polymict, clast to matrix supported and massive poorly sorted to well defined graded beds. Clasts range from

coarse sand to 100mm and are subangular to rounded. The monomict conglomerate comprises chert clasts in a siliceous siltstone matrix. Clasts in the polymict units in order of abundance are dacite and rhyolite volcanics, serpentinite, chloritized mafic volcanics, vein quartz, chert and carbonate.

Greywackes and the matrix in both conglomerate types comprises angular to subrounded grains of polycrystalline quartz, minor volcanic quartz, plagioclase, siltstone, muscovite, magnetite and minor chrome spinel (Plate 4). Probe data for the chrome spinel grains from sample No 30989 (see Appendix 4) is plotted in Fig 5 (Cr# versus Mg#) and indicates that the grains could have been derived from boninites, layered dunite-harzburgite or the HFW ophiolite.

The detrital magnetite component is associated with an aeromagnetic anomaly (Fig 3), however Leaman (1991) attributes most of this feature to buried ultramafic slices.

Siltstones are pink to green in colour (latter chlorite veined), massive to occasionally bedded but this is frequently obscured by cleavage. Cement in siltstones and greywackes is hematite, carbonate or chlorite.

Provenance for the greywacke conglomerates is similar to the underlying quartz sandstone but more varied. Sources in order of abundance included Precambrian metamorphics, felsic to intermediate volcanics, tholeiitic basalts and ultramafics.

The hematite facies sedimentary rocks contain up to 10.8% Fe_2O_3 and are interpreted to have been deposited in a shallow oxidizing subaqueous environment. Glennie (1970) considers oxide facies sediments to be indicative of an arid shoreline environment combined with post depositional conditions of +ve

Eh and high pH to preserve hematite during diagenesis. A similar sequence in the CCF has been described by Haines (1991) at Renison Bell, where thick oxide facies greywackes, carbonates and evaporites have been interpreted to have been deposited in a shallow but rapidly subsiding basin.

Alternating green (chloritic) and pink (hematitic) bands frequently occur in greywackes and siltstone in the HFW. This is interpreted to be due to post depositional reduction of hematite, rather than reflecting changes in sediment composition. Evidence for this alteration during diagenesis includes;

- colour bands are frequently bedding transgressive
- major element analysis of greywackes from DDH HR3 (Table 2), have similar levels of SiO_2 and TiO_2 in both green and pink greywackes, and indicate that there has been no change in provenance ie more basaltic or felsic.
- differences in MgO and FeO content (Table 2) are interpreted to result from the formation of chlorite at the expense of hematite and is associated with the introduction of MgO with basin brines. Meares (1980) reports diagenetic dolomitic septarian nodules in siltstone, supporting the introduction of MgO .

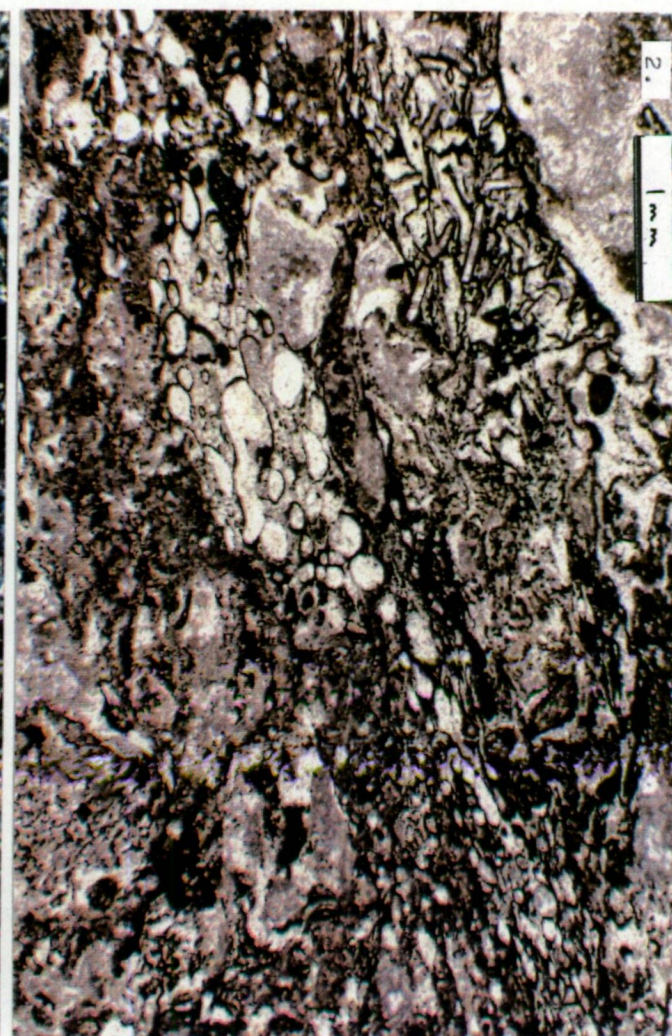
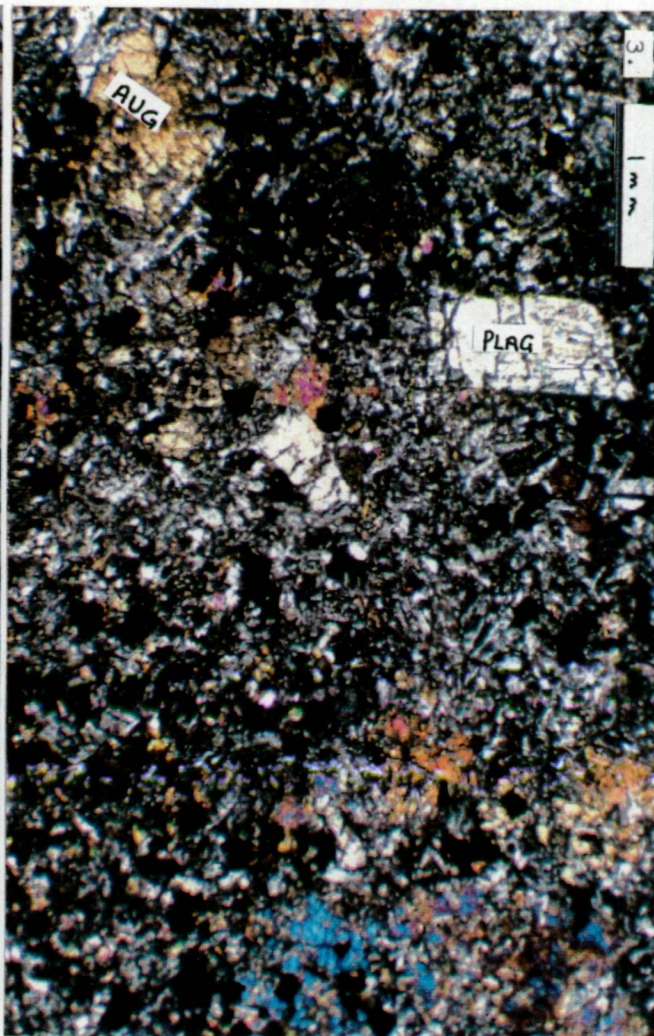
Table 2. Major element analysis of greywackes from DDH HR3

| | SiO ₂ | Al ₂ O ₃ | TiO ₂ | Fe ₂ O ₃ | CaO | MgO |
|---------------------------------|------------------|--------------------------------|------------------|--------------------------------|-------|--------|
| 32844 301.7m pink greywacke | 60.1% | 13.86% | 0.72% | 9.27% | 1.04% | 6.64% |
| 32845 302.0m green greywacke | 56.9% | 15.36% | 0.82% | 7.16% | 0.22% | 10.79% |
| 32846 322.5m pink greywacke | 56.3% | 15.51% | 0.86% | 10.82% | 0.33% | 7.38% |

PLATE 2. 31666 Henty Valley tholeiitic vesicular basalt - sericite/
pyrite altered (plane polarized light).

PLATE 3. 31683 Henty Valley tholeiitic basalt lava or sill (crossed
nicols).

PLATE 4. 30136 Henty Valley hematitic wacke - opaque hematite cement -
chrome spinel grain centre of view (plane polarized light).



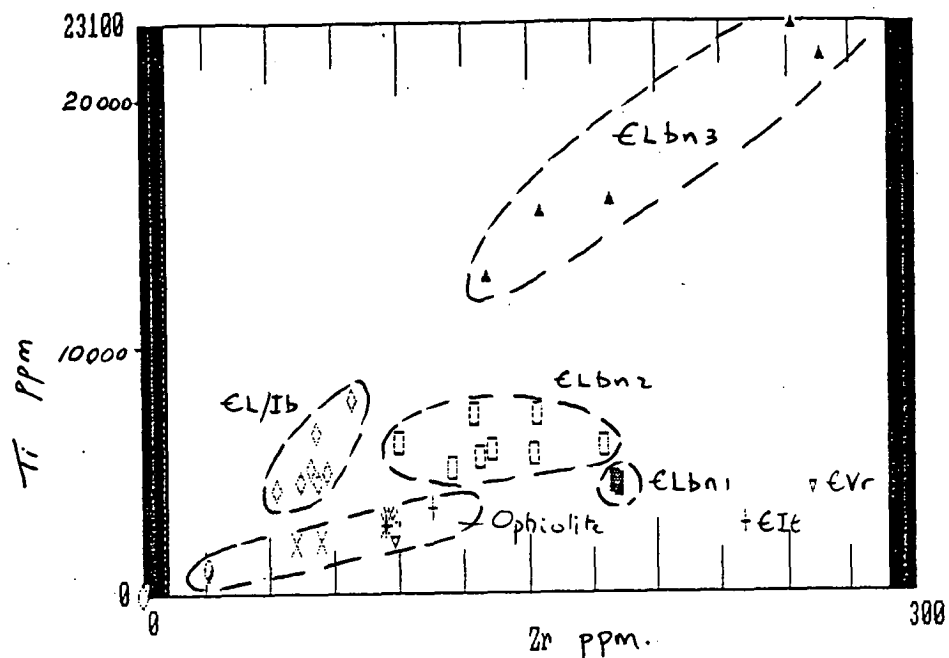


Figure 6 Ti-Zr plot, showing fields for Henty Fault Wedge lavas and intrusives. For key to symbols used see Table 2 (page 24)

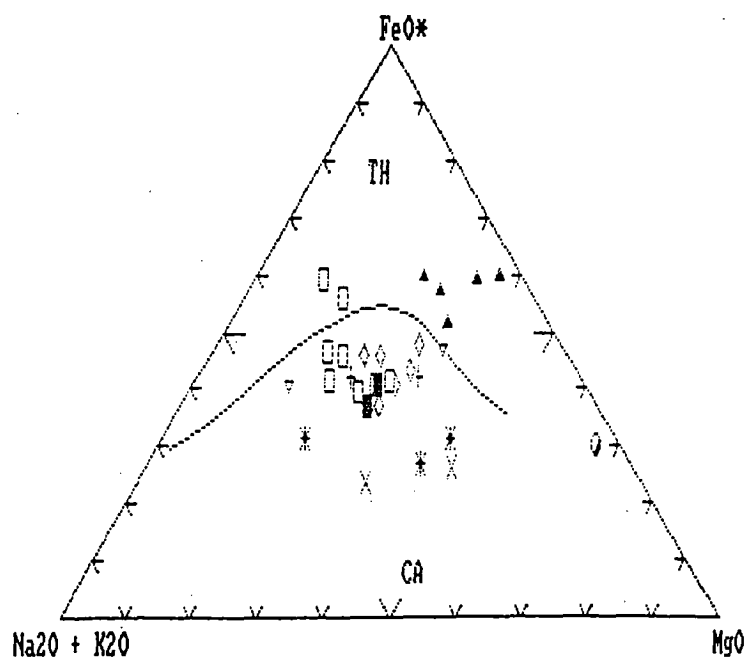


Figure 7 $\text{Na}_2\text{O} + \text{K}_2\text{O}$ - FeO - MgO plot, differentiation of tholeiite and calc - alkaline series lavas and intrusives from the Henty Fault Wedge. Fields of tholeiite (TH) and calc-alkaline (CA) compositions after Irvine and Baragar 1971. For key to symbols used see Table 2 (page 24)

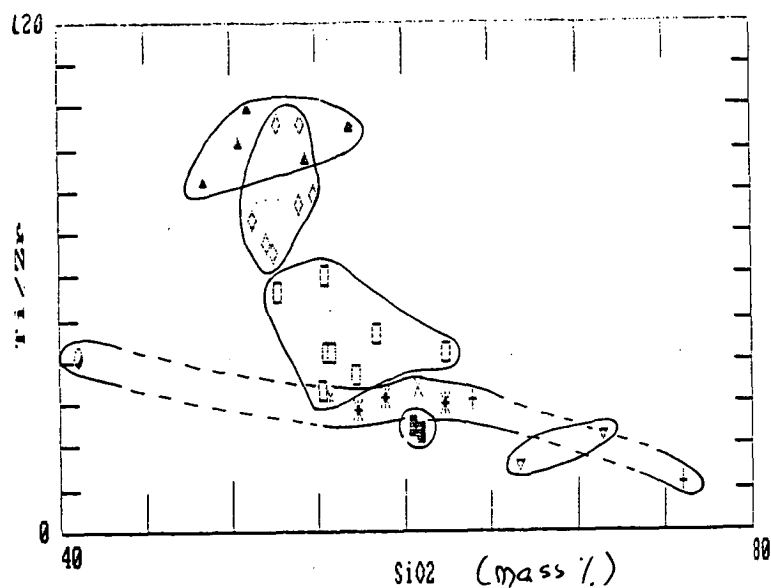


Figure 8 Ti/Zr-SiO₂ (mass %) plot for Henty Fault Wedge lavas and intrusives. For key to symbols used see Table 2 (page 24)

TABLE 2. Symbols used on geochemical plots for Henty Fault Wedge rocks

| | | |
|--------------------------------|-------|---|
| Henty Valley basaltic andesite | CLbn3 | ▲ |
| Henty Adits basaltic andesite | CLbn2 | ◻ |
| Halls Rivulet Track andesite | CLbn1 | ■ |
| Ewart Creek basalt - gabbro | CL/Ib | ◊ |
| Ophiolite complex- tonalite | CI t | + |
| " " - andesite lava | CVn1 | * |
| " " - andesite dyke | CIg | x |
| " " - gabbro | Cg | ○ |
| " " - serpentinite | Cus | ● |
| Rhyolite | CVr | ▽ |

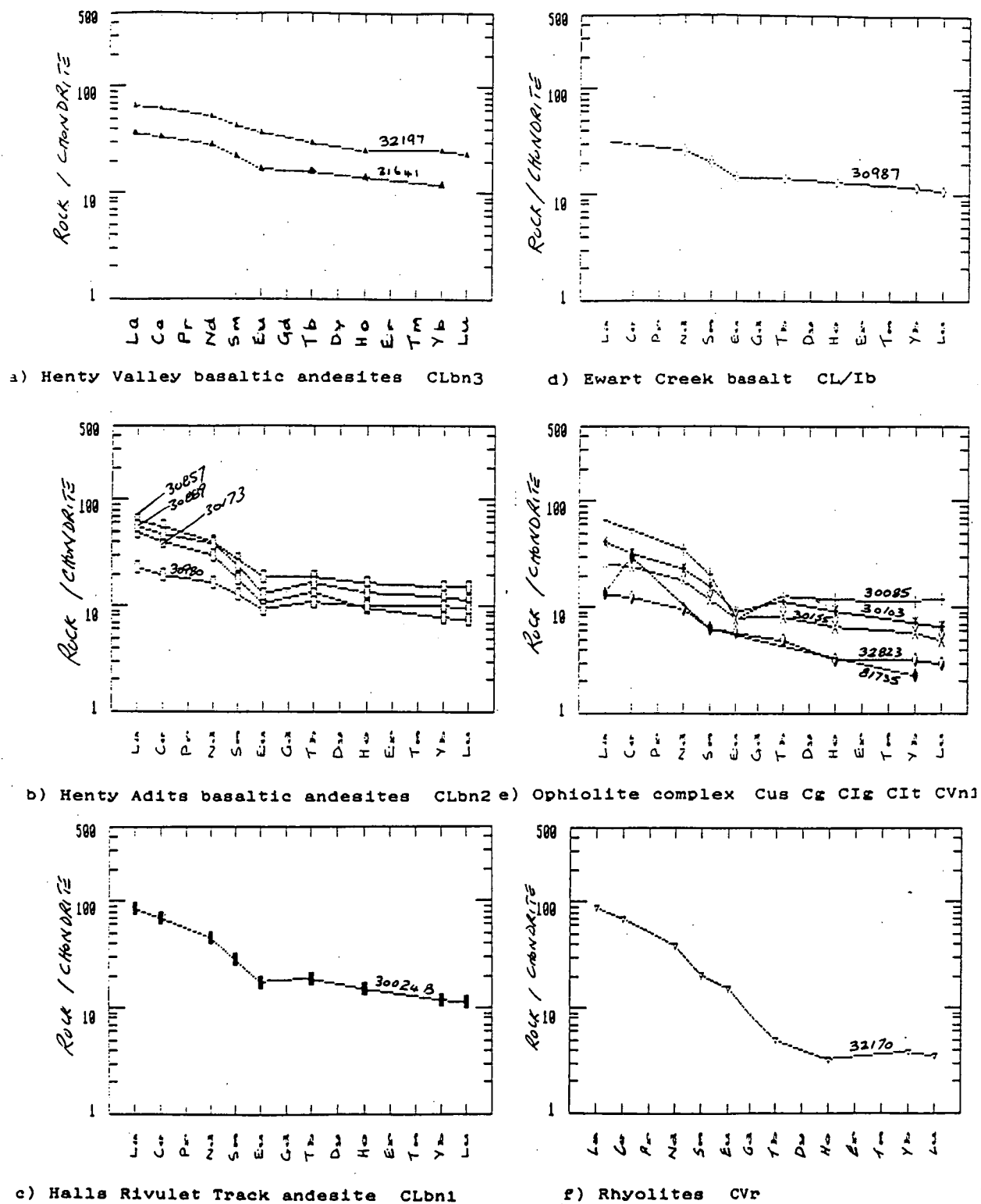
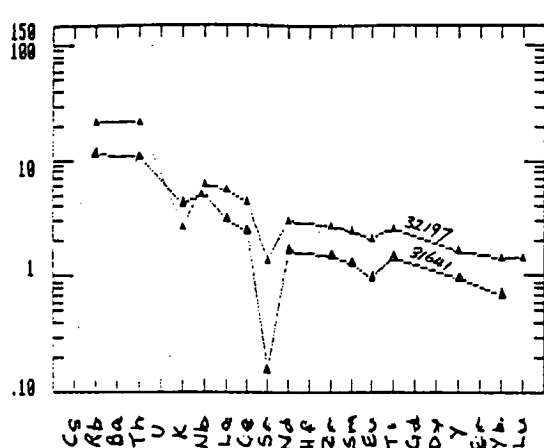
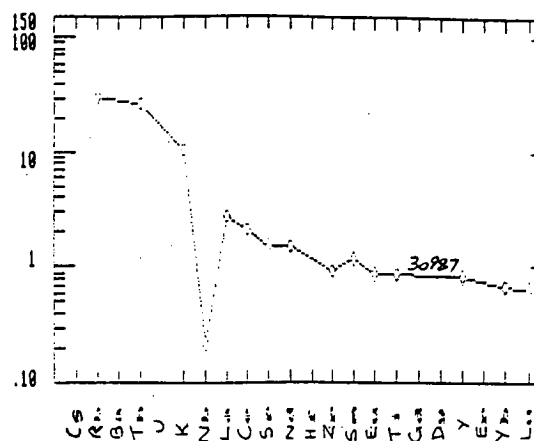


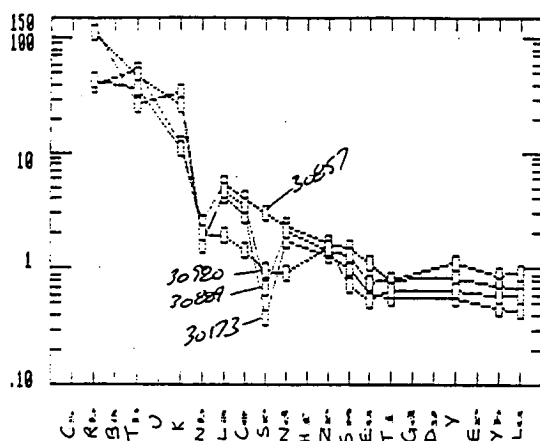
Figure 9 Chondrite-normalized REE patterns for Henty Fault Wedge igneous rocks. For key to symbols used see Table 2 (page 24)



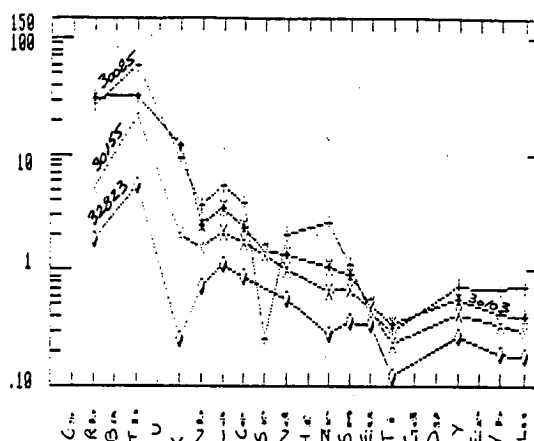
a) Henty Valley basaltic andesite CLbn3



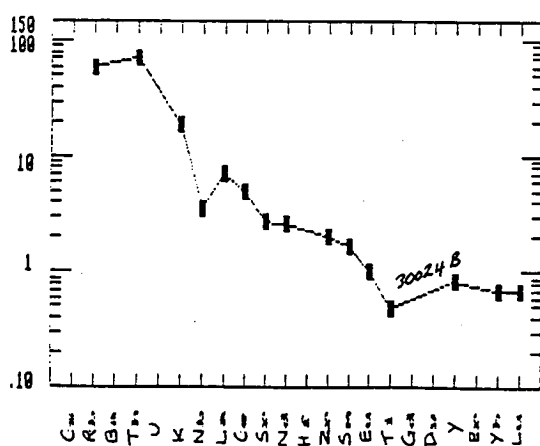
d) Ewart Creek basalt CL/Ib



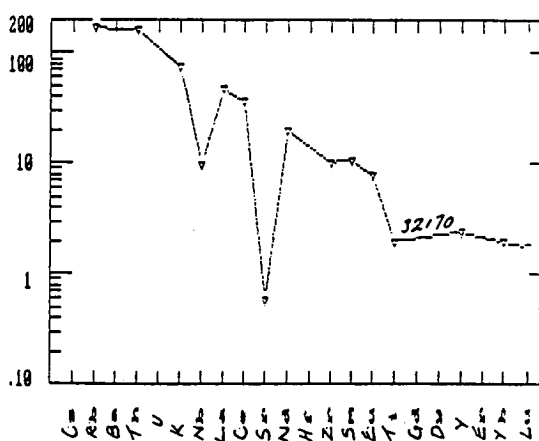
b) Henty Adits basaltic andesite CLbn2



e) Ophiolite complex Cus Cg Cig Cit CVn1



c) Halls Rivulet Track andesite CLbn1



f) Rhyolite CVr

Figure 10 PRIM - normalized geochemical patterns for Henty Fault Wedge igneous rocks. For key to symbols used see Table 2 (page 24)

5.3 HENTY ADITS SEQUENCE CSslt CLbn2

5.3.1 Introduction

The sequence, comprising basaltic andesite lavas, volcanoclastics and siltstone, is exposed on the steep slopes of the Henty River valley between the Henty Adits and the end of the Halls Rivulet track, north Henty area between 58000N - 60000N and at the Henty Valley Prospect (Fig 2). The latter two areas have been separated from the main occurrence at the Henty Adits by displacements on the White Spur Creek Fault and the South Henty Fault.

The best stratigraphic detail for the sequence is at the Henty Adits where upper and lower contacts are intersected in drilling. The base of the sequence conformably overlies hematite facies wackes (Meares, 1980). The upper andesites are overlain by felsic volcanic derived sandstone (Fig 4). This upper contact has been intercepted in DDH HR5 but the drill core no longer exists. Relationships with adjacent sequences have not been defined at the other localities.

5.3.2 Sedimentary rocks CSslt

At Henty Adits a transitional andesitic volcano sedimentary sequence 85m thick conformably overlies hematite facies wackes of the Henty Valley Sequence. Siltstone are grey (minor chloritic and hematitic), occasionally with sideritic concretions and septarian nodules (Meares, 1980). Similar carbonate nodules occur at Henty Valley in grey siltstone. These siltstones at Henty Valley contain probable Middle Cambrian age brachiopods (Corbett and Lees, 1987); this is the only biostratigraphic control within the HFW.

At Henty Adits dolomitic siltstone adjacent to the SHF host semi-massive sulfide mineralization, Meares (1980) reports 6m @ 2.88% Pb 1.61% Zn 15g/tAg from Adit No. 1. At all localities siltstones contain varying amounts of disseminated and veinlet pyrite and to a lesser extent pyrrhotite.

5.3.3 Volcanics CLbn2

Basaltic andesite - andesite occurs as laterally extensive lavas and comagmatic intrusives; at Henty Adits, drilling has intersected a true thickness of 240m. At this location there is textural evidence for the andesites being lavas: the section includes hyaloclastites, pillow lavas and flows have peperitic contacts. At other localities exposures are poor and andesites may be shallow intrusives or lavas.

In thin section basaltic andesites are variably plagioclase phyric and rarely augite phyric. Phenocrysts are frequently flow orientated in both lavas and intrusives (Plate 5). Lavas have fine grained groundmass; intrusives are interpreted on the basis of holocrystalline plagioclase groundmass. Vesicles have only been recognised at Henty Valley where they are filled with calcite and chlorite.

The association with siltstones, and the occurrence of pillows and hyaloclastites indicates that lavas were emplaced subaqueously. The depositional environment changes from shallow water hematite facies in the underlying sequence, to reducing conditions; this may be associated with increased water depth and/or more sulfidic conditions associated with volcanism. The laterally extensive nature of the lavas (3km strike extent) and their predominantly coherent nature indicates effusive emplacement distal to an eruption centre.

The Ti-Zr plot of the Henty Adits basaltic andesites (Fig 6) shows calc-alkaline trends with no increase in Ti with differentiation, however some overlap with the tholeiite field can be seen on the AFM plot (Fig 7). The plot of Ti/Zr - SiO₂ (Fig 8) define the samples as a discrete suite with minor overlap with ophiolite dykes. The andesites are medium to high K with K₂O between 1.23 - 3.84% TiO₂ 0.85-1.21% and Nb 5 - 9ppm. Relative concentrations of these elements compared to other lava suites can be seen in the spider plot (Fig 10b).

The REE show slight LREE enrichment and a flat HREE plot (Fig 9b), (La/Yb)_n range from 2.3-4.5, with maximum variation between light and heavy REE La 21.4 - Yb 3.34ppm and La 7.82 - Yb 2.32ppm.

A common feature of these basaltic andesites is the anomalous levels of Zn which ranges from 213-432ppm; the highest value recorded of 835ppm is associated with alteration and mineralisation.

On the basis of Cr content two subgroups of the basaltic andesite can be recognized, distinguishing the Henty Adits andesite (Cr 12-72ppm) from those at North Henty and Henty Valley (116-176ppm). Variation in Mg#, K₂O and REE abundance is only partially coincident with this subdivision.

5.4 HALLS RIVULET TRACK SEQUENCE CSv2 CSv CSw1 CLbn1

5.4.1 Introduction

This sequence overlies the Henty Adits basaltic andesites. The stratigraphic top and western margin is the Howards Tramway Fault and associated serpentinites (Fig 4). The sequence includes mafic-felsic derived volcanoclastics, black siltstone, basaltic andesite and basic dykes. The most extensive exposure is along the Halls Rivulet Track (Fig 2); the sequence may be in the order of a 1000m thick but the internal stratigraphy has not been defined and structural repetitions may occur.

There are marked similarities between crystal lithic sandstones and vitric siltstones in this sequence and those at Ewart Creek. Both are immature sediments derived from mafic to felsic volcanics.

5.4.2 Sedimentary Rocks CSv2 CSv CSw1

The stratigraphically lowest unit exposed in this area is an interlayered volcanoclastic sandstone and siltstone (CSv CSv2). The sandstone lacks any apparent bedding except for that defined by minor black siltstone horizons. Spherical features in the sandstone to 2mm diameter are the only macroscopic textures and may be accretionary lapilli.

In thin section the sandstone is composed of angular "shard like" elongate volcanic quartz fragments and minor zircon grains in an abundant fine quartz sericite matrix (Plate 6). Tuffaceous siltstone in thin section is very fine grained; the only distinguishable components are minor quartz and muscovite.

The volcanoclastic wackes and conglomerates (CSw1) are poorly sorted, matrix supported, crystal rich and clast poor. The matrix <4mm grainsize is composed predominantly of slightly rounded albitized plagioclase and subordinate volcanic quartz (equant grains in contrast to the underlying sandstone), augite, hornblende and FeTi oxides. Clasts are <50mm in diameter and include tuffaceous siltstone, carbonate altered dolerite and chloritized formerly glassy fragments.

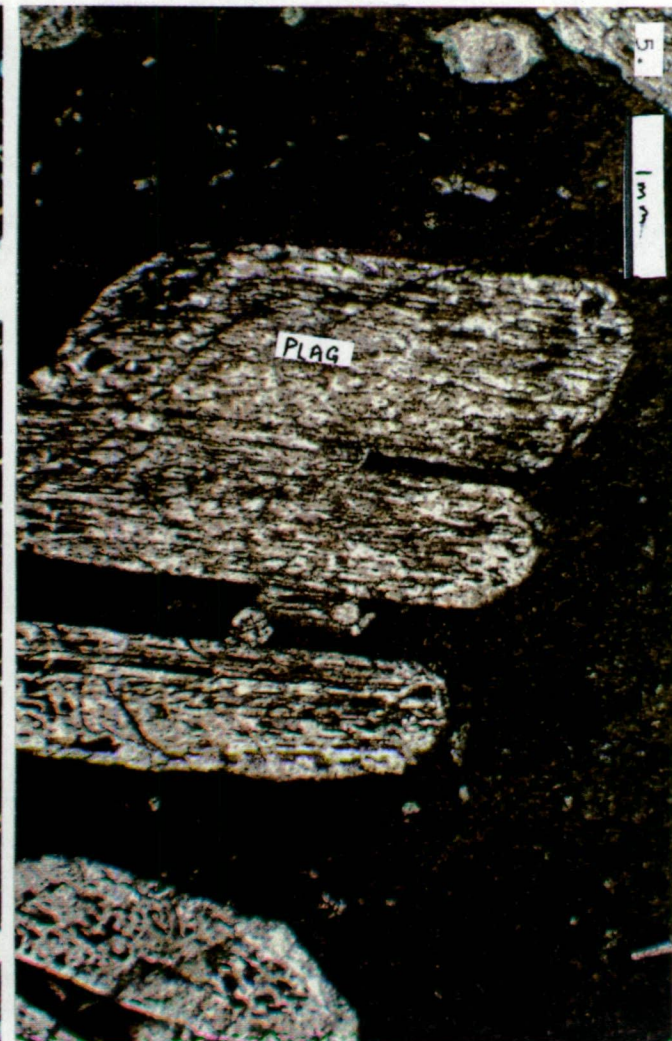
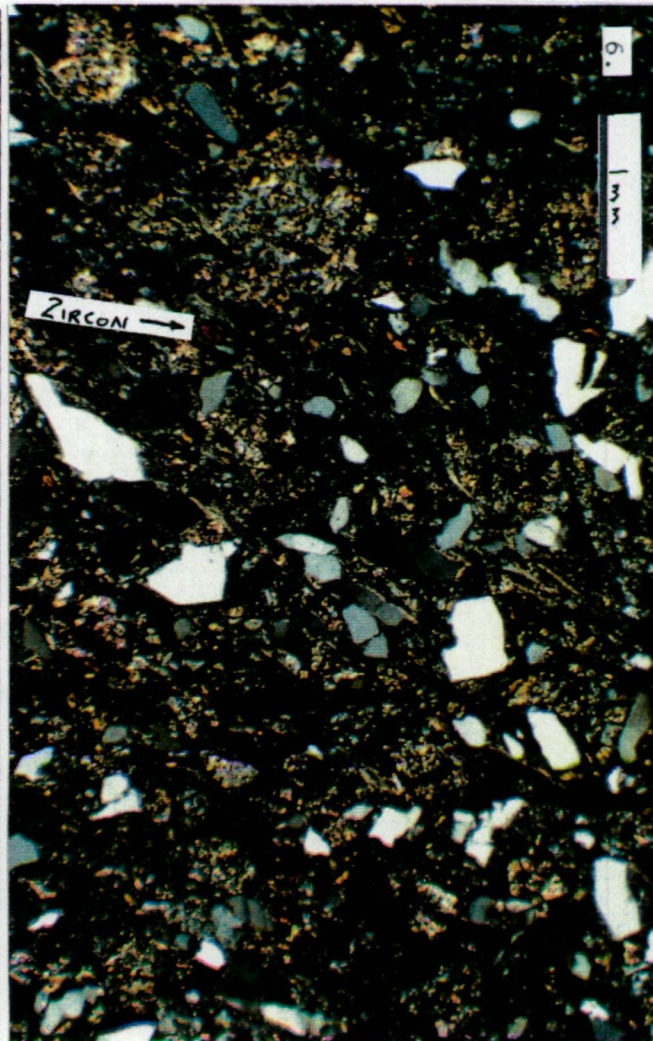
The abundant fine tuffaceous matrix and angular quartz fragments in the basal sandstone indicate derivation from explosive rhyolitic volcanism. However there is a significant lack of pumice fragments which are generally associated with this style of eruption. The volcanoclastic wackes are derived from mafic to felsic volcanics and dolerite.

The massive felsic-derived sandstone and overlying tuffaceous siltstone represent graded mass debris flow units in the order of 100m thick. The upward fining is complete in one unit which is capped by black siltstone which is considered to have been the ambient sedimentation in the basin. The graded sandstone units and the association with black siltstone indicates a subaqueous depositional environment. A similar depositional environment is envisaged for the compositionally more variable volcanoclastic wackes higher in the sequence.

5.4.3 Volcanics CLbn1

The basaltic andesites are strongly plagioclase (<3mm) and augite phyric (Plate 7) and are frequently associated with fine grained dykes of unknown affinities. On the basis of fine groundmass and float of breccias with interstitial jasper, the andesites are interpreted as lavas, although contacts with enclosing sediments are not observed. Association with mass flow volcanoclastics indicates a subaqueous emplacement environment. Total thickness of the andesite may be 200m.

- PLATE. 5. 30862 Henty Adits basaltic andesite - flow orientated
plagioclase phenocrysts (plane polarized light).
- PLATE. 6. 30141 Halls Rivulet Track volcanoclastic sandstone - angular
quartz crystal fragments - zircon grains - quartz sericite
matrix (crossed nicols).
- PLATE. 7. 30024B Halls Rivulet Track andesite - plagioclase and augite
phyric (plane polarized light).



The andesites have calc-alkaline affinities (Fig 6 and 7), are medium to high K with K₂O values between 2.12-3.24% and TiO₂ ranges from 0.72-0.75%.

The Ti/Zr - SiO₂ plot (Fig 9) separates these from the Henty Adit andesite; with some overlap with the ophiolite andesite lava and dyke field.

Normalized REE are plotted in Fig 9c and show LREE enrichment and more or less flat HREE, the (La/Yb)/N is 7.14, with La 28 and Yb 2ppm.

5.5 OPHIOLITE COMPLEX

5.5.1 Introduction

The complex is a fault bounded block on at least three sides, to the north and south splays of the Henty Fault and to the east the Howards Tramway Fault (Fig 2). In addition dismembered serpentinitized ultramafic slices occur along the NHF. The western contact is marked by a greywacke horizon which is overlain by the Ewart Creek Sequence (Fig 11), the nature of this contact is unknown but difference in metamorphic grade (lower greenschist facies in ophiolite dolerite and prehnite-pumpellyite in the Ewart Creek Sequence) between the two sequences indicates a significant erosional or faulted contact.

The unit is poorly exposed due to deep weathering, particularly the andesite lavas. The geology has been compiled entirely from float and soil type mapping.

From east to west the complex comprises:

- dunite, pyroxenite and coarse grained gabbro cumulates.
- gabbro, dolerite, andesite dykes and tonalitic plugs.

- andesite lavas, andesitic volcanoclastics
- siltstone, greywacke

When compared to lithological layering in other ophiolite sequences (Nicolas 1989), the complex is interpreted to face west. From the nature of the magnetic anomaly associated with serpentinized ultramafics in the east (Fig 3) and steep dips in greywackes the complex is interpreted to dip steeply west.

The cumulates, intrusives and lavas are considered to be a comagmatic complex on the basis of similar immobile element concentrations (Fig 9e and 10e) and the calc-alkaline affinities (Fig 7) common to all igneous lithologies.

5.5.2 Sedimentary rocks CSslt CVn1

The sedimentary rocks are subdivided into coarse grained volcanoclastics associated with the andesite lavas and siltstone/greywackes which mark the contact between the ophiolite complex and the Ewart Creek Sequence.

Volcanoclastics are matrix supported and poorly sorted. Clasts are <100mm, subrounded and include quartz-amygdaloidal andesite lava, plagioclase-phyric lava, quenched lava and plagioclase aggregates, the latter probably derived from amygdales. The matrix is composed of quartz grains, sericite and abundant hematite.

Exposures are not extensive enough to define bedforms and bed thicknesses.

These clastics are interpreted to have been in part derived by quench fragmentation from the associated andesite lavas in a subaqueous environment. However some clasts are rounded indicating transport and reworking.

The presence of hematite in these clastics may be a product of alteration as suggested by Crawford in Poltock and FitzGerald (1991) or alternatively shallow water to subaerial oxidizing conditions.

Siltstone and greywackes are relatively mature compared to the underlying volcanoclastics; and are composed of equigranular and subangular to rounded quartz grains, muscovite and subordinate sericitized plagioclase, leucoxenized FeTi oxides and chloritic fragments. The siltstone and greywackes are thinly bedded and occur as a single horizon 100m thick with a strike extent in excess of 2.5km. Components indicate a mixed provenance, dominated by metasedimentary rocks and subordinate mafic to intermediate volcanics. The relative sediment maturity, lateral strike extent and dominance of metasedimentary detritus indicates a hiatus in volcanism, and deposition in a stable subaqueous environment.

5.5.3 Lavas and shallow intrusives CVn1

The interlayered lavas and intrusives have an outcrop area of 1.75km². Textures in the lavas are variable and include quenching with "spinifex" pyroxenes (Plate 8), quartz amygdales and plagioclase phenocrysts displaying strong flow orientation. The occurrence of pillow lavas and lava breccias is inferred from andesite float with cherty interstitial material.

Intrusives are plagioclase-phyric and occasionally have a distinctive needle-like holocrystalline groundmass of plagioclase with abundant interstitial hematite.

5.5.4 Intrusive complex CIg CIt

The intrusives have an exposed area of 4.75km^2 and comprise predominantly fine to medium grained gabbro and dolerite with subordinate andesitic dykes and scattered tonalite plugs.

Dolerite and gabbro are variably plagioclase phyric (1-2mm) with a holocrystalline groundmass of plagioclase and subordinate augite (Plate 9). Plagioclase is albitized and frequently pink in hand specimen, augites are altered to chlorite-actionolite reflecting the higher metamorphic grade.

Andesite dykes are aphanitic with chilled margins. Plate 9 shows the contact between a dolerite and dyke.

Tonalites outcrop as numerous plugs and dykes, with a total outcrop area of 0.5km^2 , the largest body 0.25km^2 . These intrusives occur mainly in the southern part of the complex and around the margins. With the exception of a single dyke within the Henty Valley Sequence greywackes located at 78500E, 57760N all tonalites occur within the gabbro dolerite complex. The tonalities are difficult to differentiate from dolerites in the field, and may be more extensive than the current mapping shows.

In thin section the tonalities are equigranular to plagioclase phyric, with a groundmass of quartz, plagioclase (minor K feldspar), chloritized biotite (hornblende) and minor zircon. Quartz crystals have an irregular outline, are poikiloblastic with plagioclase inclusions and resorbed margins (Plate 10).

5.5.5 Cumulates Cg Cus

Gabbro, pyroxenite and dunite form the eastern and basal part of the complex between 5340000N and 5356500N, the Howards Tramway Fault being the bounding structure.

Elsewhere the altered cumulates occur as isolated fault slices <100m thick within the North Henty Fault (NHF), splays of the SHF at 5351800N and within ophiolite andesites at 5354000N 74700E.

Aeromagnetics (Fig 3 defines the outcrop extent of the ultramafics; in addition Leaman (1991) interprets the main body of the magnetic anomaly within the HFW between 54000N-60000N and in the SW coincident with the Ewart Creek Sequence as being associated with buried ultramafic bodies. This interpretation is queried here and the magnetic highs are interpreted to be associated with magnetite-bearing greywackes and tholeiitic basalts.

The most extensive exposure of the cumulates occurs on the Halls Rivulet Track where gradational contacts can be observed between serpentinized dunites, pyroxenites and gabbros. Ultramafics are pervasively altered to serpentinite, talc, silica and carbonate, and chrome spinel is frequently the only remnant primary mineral. Spinels from sample No. 30091 were probed, giving a Cr# between 79-82 (Appendix 4 and Fig 5). In thin sections 30091 and 216511 remnant textures indicative of cumulate olivine and pyroxenes have been interpreted by Crawford, in Poltock and FitzGerald (1991) and Joyce, in Poltock (1987).

5.5.6 Geochemistry of the ophiolite

A fractionation trend from the cumulate base to the tonalites is suggested by the variation in Mg^* ($Mg^* = Mg/Mg + Fe$) with values from 80 (gabbro) - 49 (tonalite). The sensitivity of Mg^* to fractional crystallization is established by Wilson (1989).

This fractionation trend is also reflected in the normalized REE plots for different rock types (Fig 9e). This pattern in the REE is due to the incompatible nature of these elements and their progressive enrichment during fractionation in the residual melt (Cox et al, 1979).

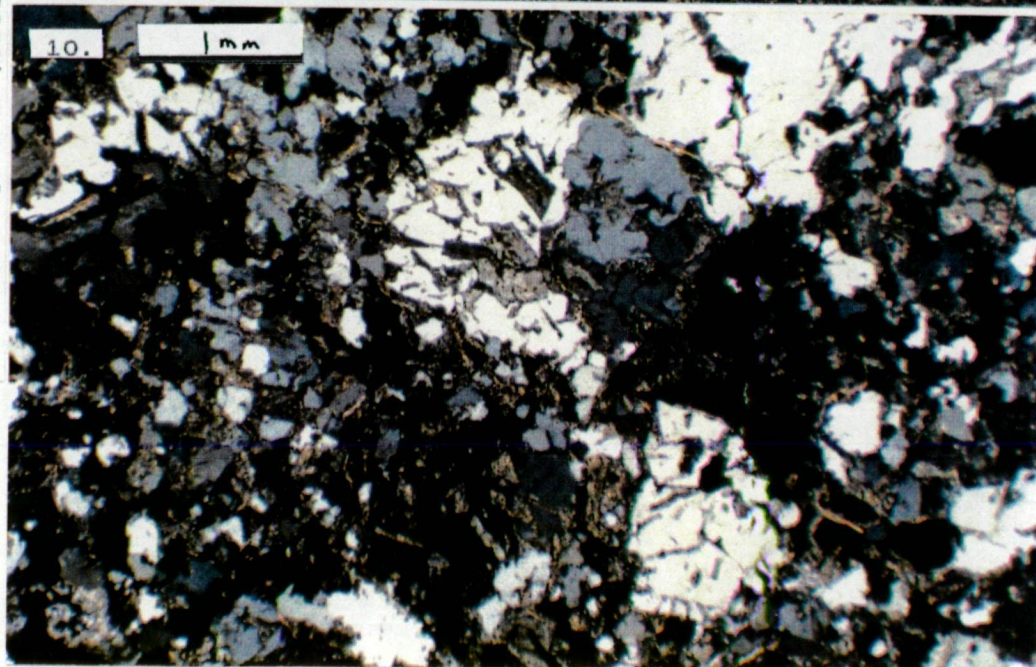
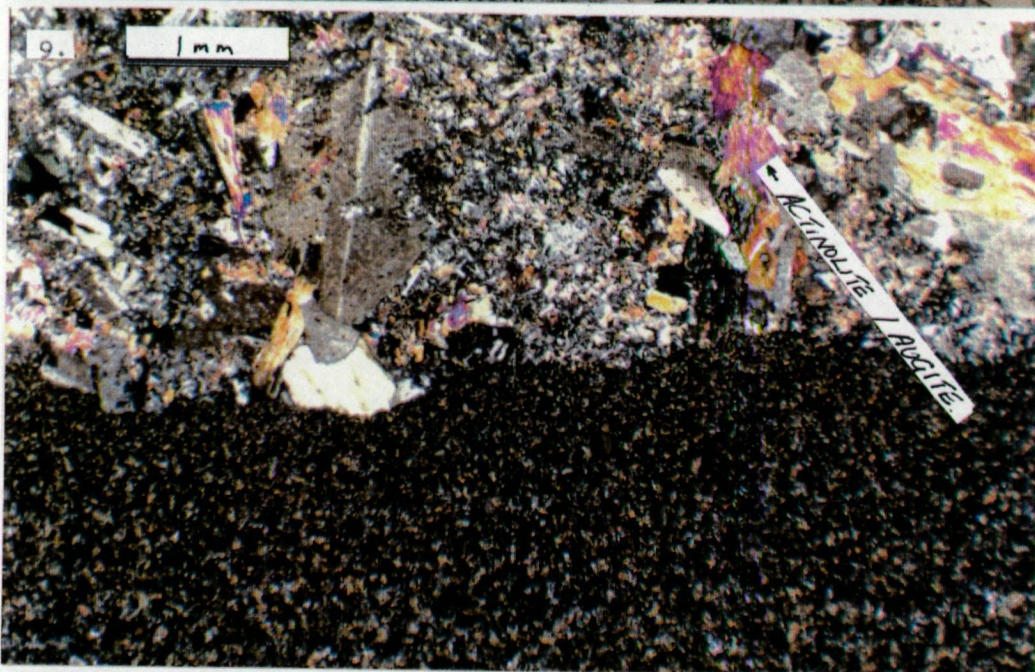
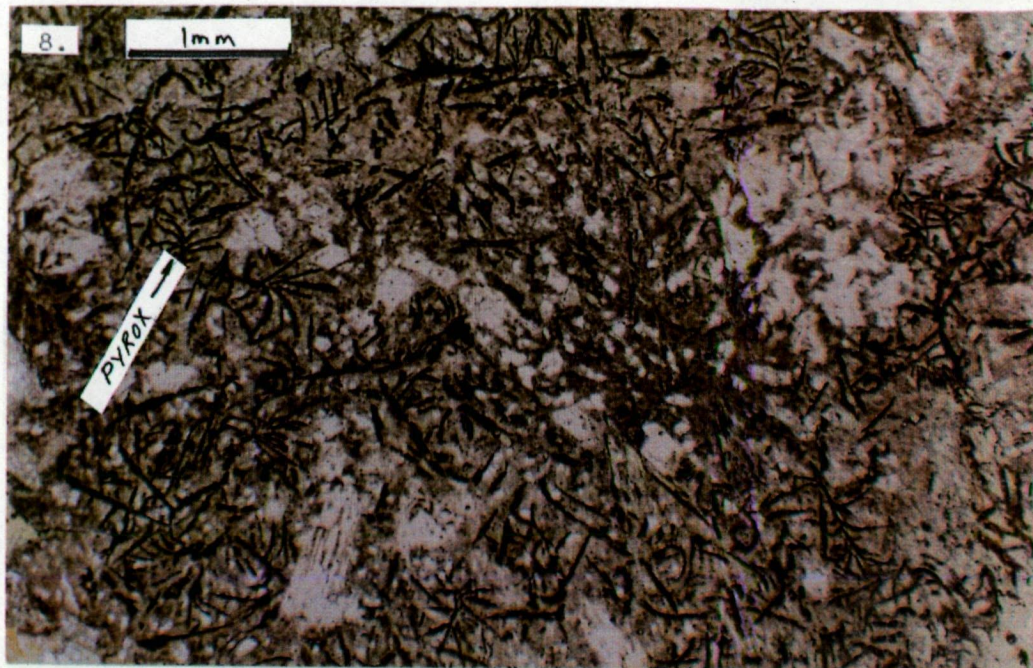
All rock types in the complex have slight LREE enrichment and nearly flat HREE plots, cumulates have the lowest concentrations of REE and there is a progressive enrichment through the andesites to tonalites. $(La/Yb)/N$ range from 4.22 for cumulate gabbro to 5.90 for tonalites.

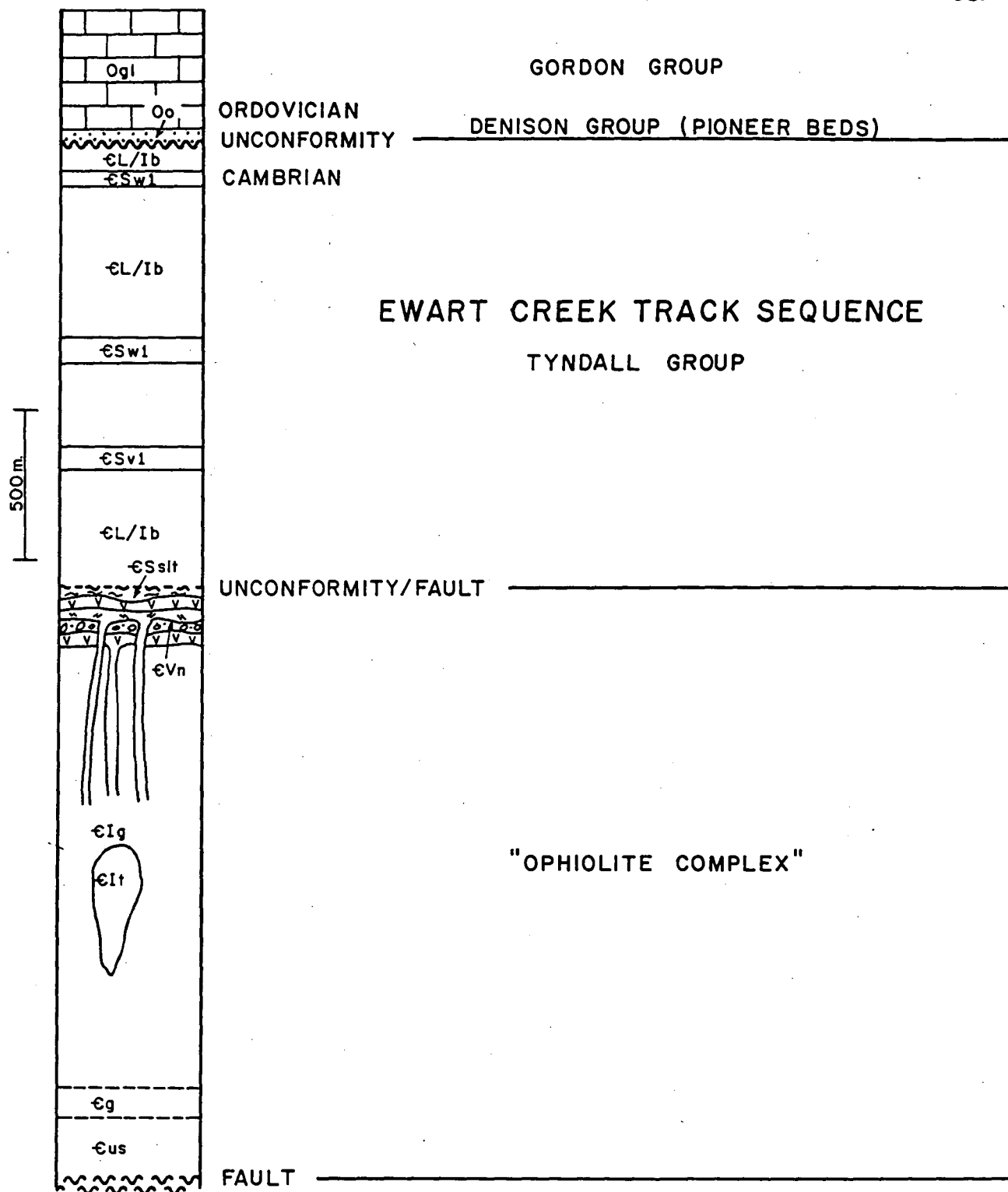
Calc-alkaline affinities of the complex can be seen in the Ti-Zr plot (Fig 6) with progressive reduction of Ti with fractionation from gabbros with 41% SiO_2 - TiO_2 0.18% to tonalites with 76% SiO_2 - TiO_2 0.49% (Fig 8). The calc-alkaline affinities are confirmed by the AFM plot (Fig 7).

PLATE 8. 30103B Ophiolite Complex andesite lava - quenched pyroxene (plane polarized light).

PLATE 9. 30155 Ophiolite Complex - chilled contact between dolerite and andesitic dyke - actinolite development in dolerite pyroxenes (crossed nicols).

PLATE 10. 30085 Ophiolite Complex tonalite intrusive - poikiloblastic quartz (crossed nicols).





Refer to 1:25000 Legend

**PASMINCO EXPLORATION**

A Division of Pasma Australia Limited

COMPILED: R.A.P.

DATE: 27-6-'92

DRAWN: N.W.D.S.

REF.:

REVISIONS:

DRAWING No.

SCALE



FIG. No.

12

STRATIGRAPHIC SECTION
WESTERN HENTY
FAULT WEDGE

5.6 EWART CREEK TRACK SEQUENCE CSv1 CSw1 CL/lb CIg

5.6.1 Introduction

This sequence is located in the western portion of HFW (Fig 2). The nature of the eastern contact with the ophiolite complex is unknown, in the west the sequence is unconformably overlain by the basal Ordovician sandstone and conglomerates (Fig 11). This western contact is obscured by fluvioglacial in the study area, but an unconformity has been described 2km to the SW by Baillie and Corbett (1985) (see Fig 12). Alternatively this contact has been interpreted as faulted by Keele (1991) and Leaman (1991).

The sequence comprises a comagmatic suite of basalt lavas, dolerite sills and gabbro plugs. These are interlayered with tuffaceous siltstone and coarse grained volcanoclastic sandstone and minor conglomerates. In the south, near the Zeehan Highway the sequence is dominated by tuffaceous siltstone and associated dacitic volcanics with minor fine grained basalt. Maximum thickness of the sequence is 1500m, however some overturning and possible isoclinal folding may occur.

5.6.2 Sedimentary rocks CSv1 CSw1

The similarity with volcanoclastics in the Halls Rivulet Sequence has already been noted.

Tuffaceous siltstone horizons are up to 50m thick, lack internal bedding and have a strike extent of at least 2km. In thin section the siltstones are composed of fine grained (presumably) sericite and <1% fine grained quartz and muscovite. On the Zeehan Highway section, graded felsic mass debris flow units with

cherty tops are exposed. Graded units are between 10-30m thick.

Volcaniclastics range from coarse crystal-rich sandstone to clast supported polymict conglomerate. Clasts are generally <20cm diameter and include dolerite, gabbro, quenched and vesicular basalt and flow oriented plagioclase-rich basalt. Clasts are subrounded to angular, some of the latter a product of quench fragmentation (perlitic textures). The conglomerate matrix and sandstone is composed predominantly of albitized plagioclase and subordinate pyroxene, quartz and FeTi oxides. Lithic fragments in the sandstone are similar to those in conglomerates.

Clastics in the western area have a distinctive alteration banding of alternating pink albite and green chlorite rich layers, the banding is parallel to bedding.

The volcaniclastics are immature, rapidly deposited, derived from basic to felsic volcanics and fine grained basic intrusives.

5.6.3 Lavas and intrusives CL/Ib Clg

Lavas and intrusives range from basalt to basaltic andesites and are plagioclase phyric to variably augite phyric, with abundant FeTi oxides. Intrusives are porphyritic with holocrystalline groundmass; chilled margins have been observed at 51075E in the Henty River. Textures in extrusives include lobate/pillow like contacts with sedimentary units, vesicles, hyaloclastite and flow breccia margins. These textures are best observed in DDH BR1 (Corbett 1985).

Analyses from eight samples of extrusive and intrusive phases plots in a coherent group in the Ti/Zr - SiO₂ diagram (Fig 8) indicating the comagmatic nature of

the suite.

The Ti-Zr plot (Fig 6) defines the tholeiitic affinities with Ti enrichment with differentiation however on the AFM plot (Fig 7) samples straddle the tholeiite and calc-alkaline fields. Element ranges include TiO_2 0.42-1.60%, Nb 0.8-3.2ppm (Fig 10d); the low Nb content is a distinctive feature of the suite which has been noted previously by Crawford et al (1992). Two subgroups based on Cr content occur (<40ppm and 190-206ppm); the subgroups are not obviously associated with differences in lithotypes.

Chondrite-normalized plots of the REE are nearly flat with slight LREE enrichment (Fig 9d). A considerable range of REE values exist for the tholeiites from La 2.9-Yb 1.8ppm to La 52.1 - Yb 3.9ppm (Jenkins, 1990), however when plotted all samples have similar subparallel trends.

The tholeiites are interpreted to have been fed by gabbroic plugs, the SHF acting as a conduit for this magmatic activity. Most of the basalt and dolerite bodies are interpreted to be shallow sills with only a small proportion extruded as lava.

5.7 QUARTZ-PHYRIC RHYOLITE CVr

Dacite to rhyolite volcanics and volcanoclastics occur within the South Henty Fault and White Spur Creek Fault (WSCF) zones on the eastern flanks of the HFW (Fig 2). The two main bodies are 200m wide, located between 53000-53500N and 59000-60000N in the SHF, the latter occurrence is apparently interlayered with volcanoclastic wackes which have lithological similarities to the HFW rocks. The WSCF occurrence at 58500N 79040E is only a few metres wide.

Apart from occurring as fault slices the rhyolites have several features in common:

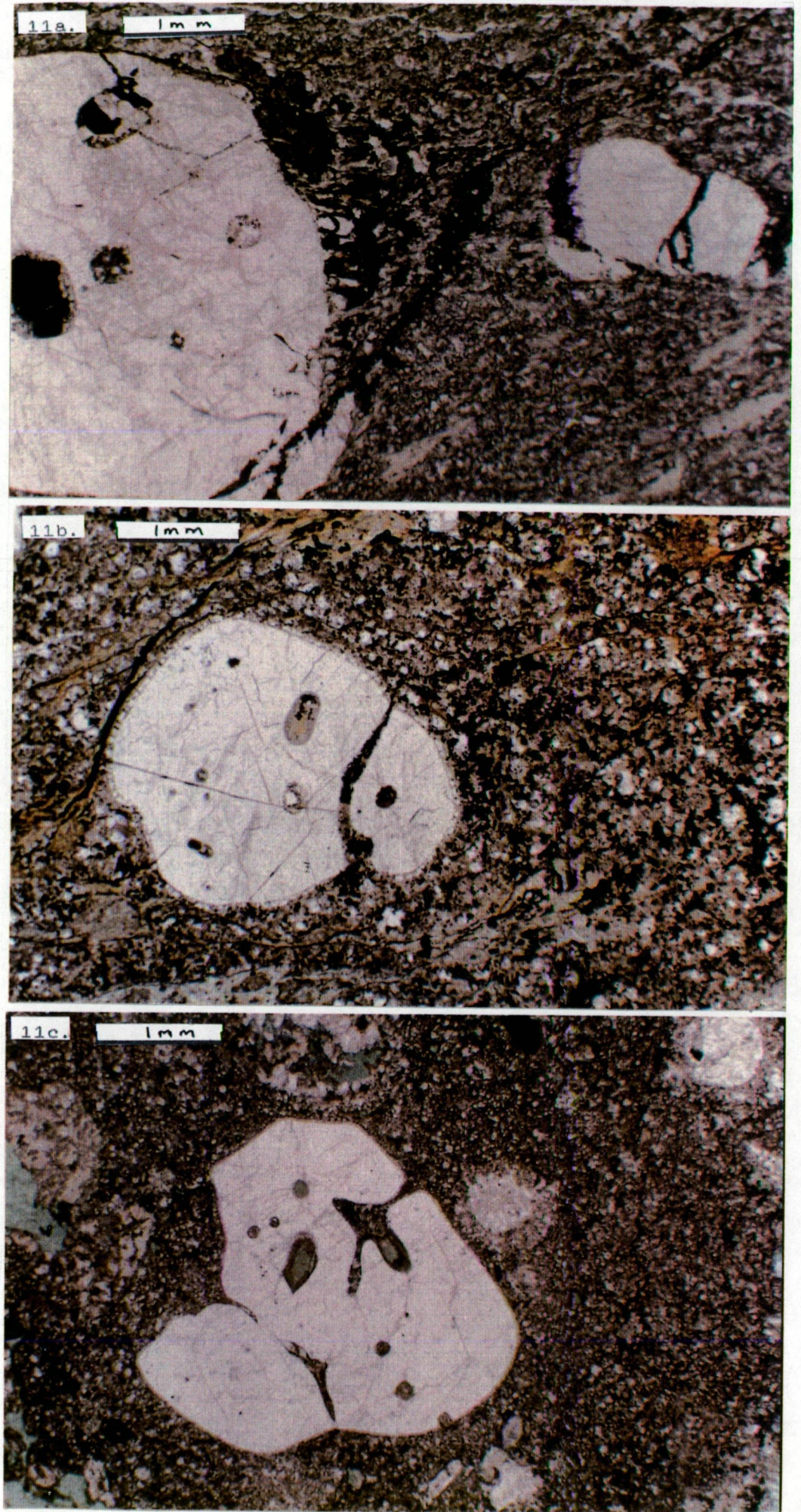
- lavas are sparsely quartz/phyric with subordinate feldspar.
- quartz phenocrysts to 3mm diameter have reaction rims and melt inclusions (Plate 11a-c).
- devitrified groundmass of fine grained quartz feldspar.
- pervasive calcite, sericite alteration.

Major element analysis is available for sample No. 30099 and major, trace and REE elements for sample No. 32170 (Fig 9f and 10f). Due to the intense alteration (AI=94) of No 32170 the mobile elements will not reflect primary levels. However the Ti-Zr plot (Fig 6) indicate calc-alkaline affinities. Anomalous levels of Cr (up to 638ppm) may reflect the presence of Cr micas but this has not been investigated.

The rhyolites are interpreted as fault displaced slices of porphyries in the Yolande River Sequence (YRS). One of these bodies has been truncated by the SHF at 5352000N (Fig 2).

PLATE.

11. Dacite - rhyolite quartz porphyries (plane polarized light)
- a) 32170 from the White Spur Creek Fault within the HFW
- b) 30099 from within the South Henty Fault at 53000N
- c) 30072 Yolande River Sequence adjacent to the SHF



5.8 LITHOFACIES SUMMARY

The HFW comprises three and possibly four separate fault juxtaposed domains, the relationships between the domains are shown in Figs 4 and 11.

Lithologies within the HFW are quite distinct from those to the east and west, this can be clearly demonstrated in geological mapping (Fig 2) and aeromagnetics (Fig 3).

All sequences within the HFW strike north-south and dip and young to the west. From east to west the fault juxtaposed domains are:

1. Quartz phyric rhyolites, pervasively sericite carbonate altered, occurring as thin slices within the SHF and WSCF. The rhyolites are similar to porphyries within the Yolande River Sequence, some of which have been truncated by the SHF.
2. Henty Valley Sequence (HVS) - Henty Adits Sequence (HAS) - Halls Rivulet Track Sequence (HRTS). These three sequences are bound by the SHF in east and Howards Tramway Fault in the west. Each sequence has a distinct sedimentary and volcanic association.

The HVS is considered to be the stratigraphic base in the HFW and consists of hematitic greywacke and conglomerate, quartz muscovite sandstone, chert and tholeiitic basaltic andesite. Based on drilling at Henty Adits the HVS is disconformably overlain by the Henty Adits Sequence which comprises basaltic andesite (transitional between calc-alkaline and tholeiitic) and siltstone which host subeconomic Pb Zn Ag mineralization. The HRTS overlies the HAS, the sequence comprises fine to coarse grained

quartz feldspar lithic volcaniclastics and plagioclase augite porphyritic calc-alkaline andesite. The HRTS is in faulted contact with serpentinized ultramafics of the ophiolite complex.

3. The HFW ophiolite complex comprises a basal serpentinized ultramafic cumulate and coarse grained gabbro. The cumulates have a gradational contact with a complex of gabbro, dolerite, andesite and tonalite intrusives. The intrusives are capped by andesite lavas and volcaniclastics.
4. The Ewart Creek Track Sequence (ECTS) is located west of the ophiolite complex; the nature of the contact between the two units is unknown but differences in metamorphic grade would indicate that it is either faulted or unconformable. The ECTS comprises tholeiitic basalt, dolerite and gabbro with interlayered volcaniclastics. Tholeiites occur mainly as sills with minor pillowed lavas. Volcaniclastics range from fine to coarse grained and have strong lithological similarities to those in the HRTS.

6. LITHOLOGICAL AND GEOCHEMICAL EQUIVALENTS OF HENTY FAULT WEDGE SEQUENCES IN WESTERN TASMANIA

6.1 DEFINITION OF REGIONAL UNITS IN THE WESTERN TASMANIAN CAMBRIAN

1. The Crimson Creek Formation was defined by Taylor (1954) as a succession dominated by mudstone with volcanoclastic and lava horizons, overlying the eo-Cambrian Success Creek Group sediments. The basalts are tholeiitic and turbidite oxide facies with carbonate horizons (Brown, 1986) and evaporite horizons (Haines, 1991).
2. Mafic - ultramafic complexes occur as fault dismembered slices throughout the western part of the Dundas Trough. The complexes are composed of cumulates, gabbro and tonalite intrusives, basalt and andesite lavas. Orthopyroxene is dominant in cumulates and the lavas form two groups, low Ti basalts and high Mg andesites/boninites (Brown, 1986).

The mafic-ultramafic complexes were emplaced as thrust slices either within or onto the eo-Cambrian Crimson Creek Formation; and on this basis they are dated as post early Cambrian. The presence of ultramafic detritus in the middle Cambrian Dundas Group places an upper age limit on emplacement (Brown, 1986).

3. Western Volcano Sedimentary Sequence (WVSS) defined by Corbett and Lees (1987) interfingers with the CVC along its western and northern margin. The sequence comprises shale, vitric tuff, volcanogenic turbidite, quartz wacke sandstone; with mixed provenance including felsic volcanics,

Precambrian metasediments and ultramafics.

Quartz feldspar phyric intrusives and andesites occur within the sequence. The andesite lavas have been included in Suite III of the MRV by Crawford et al (1992).

The WVSS poses a problem for regional correlation due to disruption by the Henty Fault; forming three subdivisions, the Yolande River Sequence (YRS), the Henty Fault Wedge and the Dundas Group. A fourth subdivision, the Mt Charter Group, is located in the Que-Hellyer area to the north.

4. The CVC are predominantly felsic to intermediate volcanics, with minor basalts and subvolcanic granitoids (Corbett 1989). There is an interfingering association with the WVSS and Tyndall Group.
5. The Tyndall Group is defined by Corbett et al (1974) as a sequence of crystal tuff, lava, breccia, shale and volcanoclastic conglomerate. The group overlying the mineralized volcanics and underlying the Cambro Ordovician Denison Group siliciclastics in the Queenstown area. At Lynchford, the Tyndall Group is apparently overlying the YRS (Corbett, 1979 and Dower, 1991).

A late middle Cambrian fauna has been described in the basal Tyndall Group in the Comstock Valley (Corbett 1989).

6.2 PREVIOUS CORRELATIONS OF SEQUENCES IN THE HENTY FAULT WEDGE

The first detailed appraisal of HFW was by Meares (1980), whose work concentrated on the sequence immediately west of the SHF in the central portion of the HFW. The volcanosedimentary sequence was correlated with the Crimson Creek Formation on the basis of a thick unfossiliferous sequence of hematitic siltstone and minor carbonates, the association with ultramafics and the relatively minor proportion of volcanics. The calc-alkaline affinities of the andesite lavas and their similarities to MRV in the Queenstown area were also recognised.

In 1987, Corbett and Lees on the basis of mid Cambrian fossils in the SW sector of the HFW, considered the sequence as a partial time equivalent of the Dundas Group. It was also recognised by them that the fault bound sequence was quite unlike similar aged sequences to the N and S, and proposed significant fault movement which had juxtaposed different terranes.

Keele (1991) in a report on structural domain mapping, notes a lithological affinity of the HFW sequence with the base of the Yolande River Sequence in the South Queenstown area.

Crawford et al (1992) assigns HFW lithologies to one of four regional subdivisions of the WVSS. More specifically the calc-alkaline andesites at Henty Adits and Halls Track are included in their Suite I of the MRV and tholeiitic basalts in the Ewart Creek Sequence are included in Suite IV of MRV. The Suite I andesites have similarities to medium - high K orogenic andesites within the Dundas Trough, and are compared to the Que-Hellyer footwall volcanics.

Tholeiitic rocks of Suite IV include both intrusive and extrusives ranging from gabbro to basalt and belong to the Henty Dyke Swarm.

6.3 CORRELATION OF SEQUENCES IN THE HFW

6.3.1 Henty Valley Sequence

This sequence represents the apparent stratigraphic base in the HFW, comprising tholeiitic basaltic andesites and greywackes which can be correlated with either the lower Cambrian Crimson Creek Formation or the post collisional, post ultramafic WVSS - Dundas Group (Miners Ridge Sandstone and Animal Creek Greywacke).

Correlation with the CCF is based on:

- basaltic andesites are tholeiitic, have nearly flat normalized REE plots (Fig 13) and have high TiO₂ (HFW 2.13 - 3.84%) content (Brown, 1986).
- Volcanics are associated with biogenic cherts. A similar association exists in the eo-Cambrian Smithton and Dial Range Troughs (Saito et al, 1988).
- wackes are turbiditic and predominantly oxide facies.

Conflicting evidence against the CCF correlation includes:

- occurrence of detrital chrome spinel grains in the greywackes with Cr# similar to those in the ultramafics - boninites (Fig 5). These ultramafics are considered by Crawford and Berry (1991) to post date the CCF.
- presence of felsic volcanic detritus in greywackes and conglomerates. This has not been recognised elsewhere in the CCF (Brown, 1986) and felsic volcanism is considered to post date the CCF in the Dundas Trough.

Alternatively the unit can be correlated with the post ultramafic, post collisional Miners Ridge Sandstone (MRS) and Animal Creek Greywacke (ACG). The sandstone and greywacke are composed of detritus derived from Precambrian quartzose metamorphics and chrome spinel bearing ultramafics. The MRS overlies a tholeiitic basalt at Lynchford and represents the base of the WVSS in the southern part of the MRV (Dower, 1991), the ACG possibly overlies the CVC at Bulgobac and is the base of the WVSS in this area (Barwick, 1991 and Corbett and Komysan, 1989).

Correlation with the MRS and ACG is based on:

- wackes primarily derived from Precambrian quartzose metasediments.
- detrital chrome spinels have similar Cr# indicating a boninitic source (Fig 5).
- wackes underlie Suite I calc-alkaline andesites of Crawford et al (1992) at Henty Adits and in the Que-Hellyer area (Corbett and Komysan 1989).

This apparent conflict in correlation and tectonic setting for the Henty Valley Sequence can be resolved if the sequence is considered as representing a continuous transition, with the intermixing of ultramafic detritus with the final phases of CCF rift volcanism and initiation of the felsic MRV volcanism. This model poses considerable difficulties in the form of contemporaneous extensional (CCF rift volcanics) and compressional (obducted ophiolite) tectonic regimes in the one terrane.

6.3.2 Henty Adits Sequence

The andesites have been previously correlated on the basis of chemistry with the Que-Hellyer footwall sequence by Corbett (1989) and more recently by Crawford et al (1992), including them in Suite I of the MRV. The correlations included the Halls Rivulet Track andesites which are discussed separately in this study.

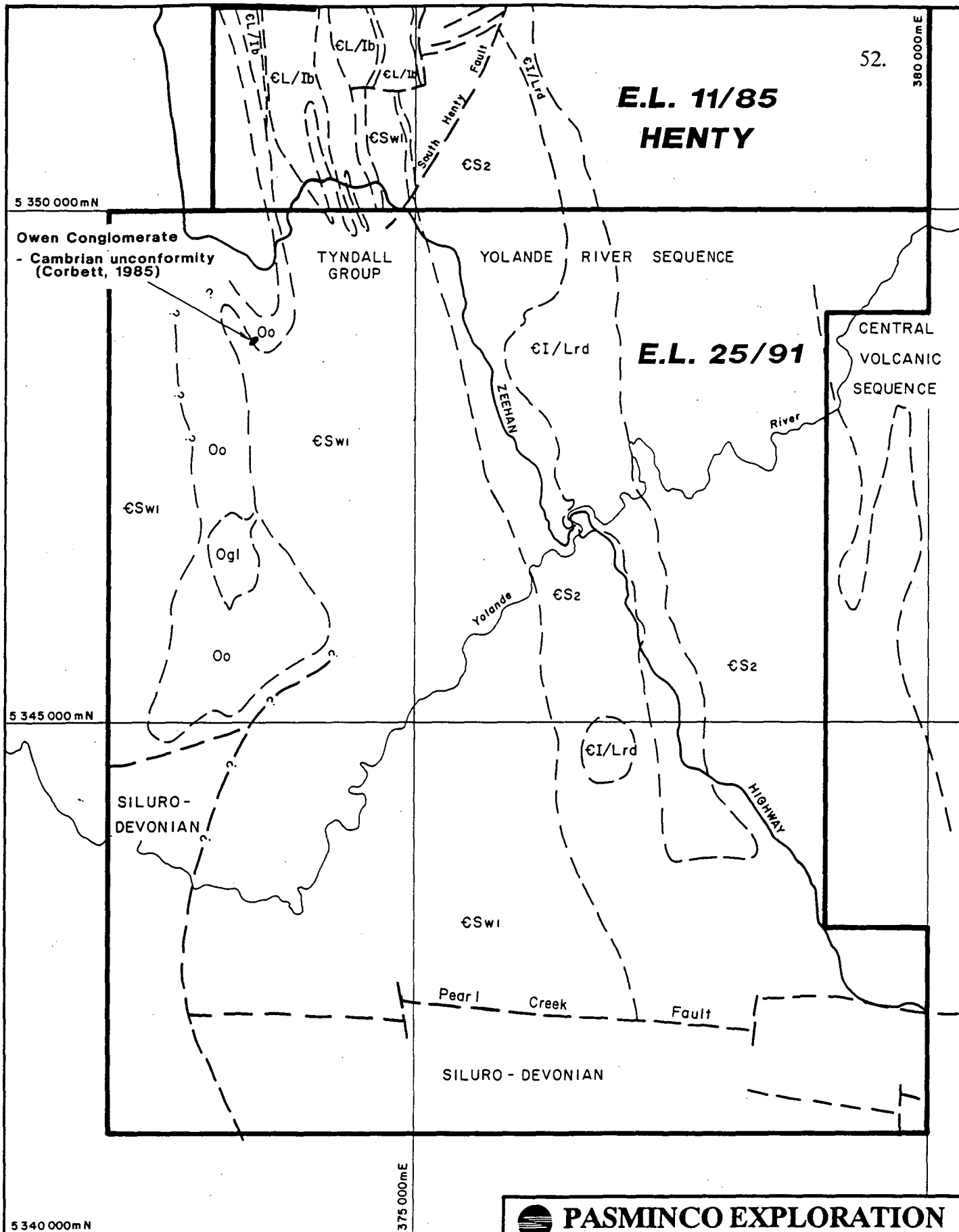
The Suite I correlation may be valid but there are significant differences between the Henty Adits basaltic andesites and other andesites in Suite I. These differences include:

- Henty Adits rocks plot between the fields of Suite I, III and IV on the Ti/Zr-SiO₂ plot (Fig 14).
- Suite I rocks have >58% SiO₂ (Crawford et al, 1992) whereas the Henty Adit rocks are basaltic andesites with 53-58% SiO₂.
- Henty Adit rocks are transitional between calc-alkaline and tholeiites (Fig 7) whereas Suite I has calc-alkaline affinities (Crawford et al, 1992).
- all basaltic andesites of the Henty Adits Sequence are plagioclase phyric and never pyroxene phyric, the least evolved rocks in Suite I are augite plagioclase phyric (Crawford et al, 1992).

More specifically the Henty Adits basaltic andesites have been compared with the Que-Hellyer footwall andesites (Corbett, 1989), geochemistry of the Que-Hellyer rocks is discussed in Corbett and Komyshan (1989). However there are significant geochemical differences between the two andesites which are listed in Table 4:

Table 4. Geochemical differences between Henty Adit Sequence basaltic andesite and Que Hellyer footwall andesites.

| | Que/Hellyer | Henty Adits |
|----------------|--------------------|--------------------|
| P_2O_5/TiO_2 | 0.32-0.76 | 0.15-0.16 |
| Al_2O_3 | 13-16% | 16-20% |
| Cr | 210-600ppm | 12-176ppm |



DATA SOURCE

Dept. of Mines - 1:50,000
Strahan and Lyell Sheets

Poltock - EL11/85



PASMINCO EXPLORATION

A Division of Pasminco Australia Limited

COMPILED: R.A.P.

DATE: July, 1992

DRAWN: G.M.B.

REF.:

REVISIONS:

DRAWING No.

**E.L. 11/85 - YOLANDE JV
E.L. 25/91 - YOLANDE RIVER JV
INTERPRETIVE GEOLOGY
STRATIGRAPHIC
RELATIONSHIPS BETWEEN
E.L.11/85 (Henty) AND E.L.25/91**

SCALE 1:50,000

0 1 km

FIG. No.

12

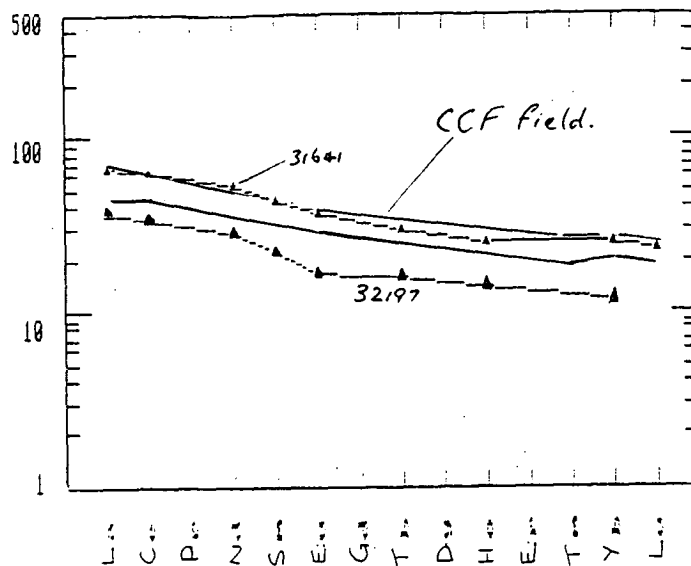


Figure 13 Comparison of chondrite normalized REE plots for Henty Valley tholeiites and Crimson Creek Formation tholeiites (from Brown, 1986)

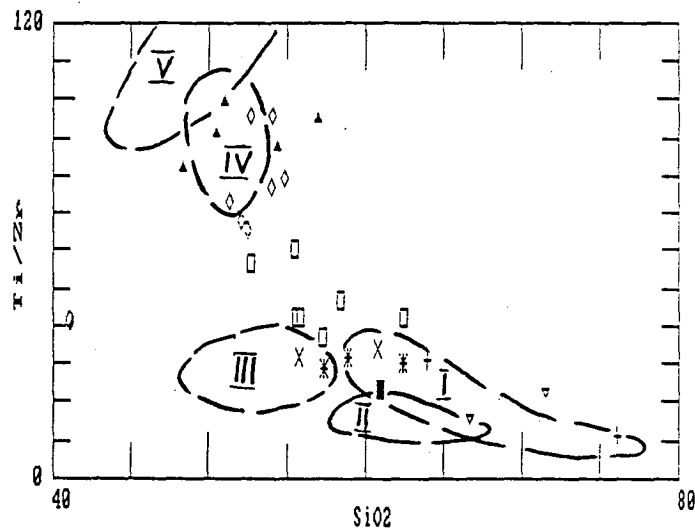


Figure 14 Ti/Zr - SiO₂ (mass %) plot, comparison of HFW igneous suites with Mt Read Volcanic Suites I - V from Crawford et al (1992), fields for Suites I - V are shown

6.3.3 Halls Rivulet Track and Ewart Creek Sequences

Within the HFW two sequences, the Ewart Creek and Halls Rivulet Track are considered Tyndall Group correlates on the basis of the nature of volcanics, petrology and geochemistry of igneous lithologies and in the case of the Ewart Creek Sequence, proximity to Denison Group siliciclastics. The two sequences have similar volcanics but contrasting igneous lithologies and structural associations. Despite these differences the correlation may be valid.

The Halls Rivulet Track Sequence is located in the central part of the HFW, dips and youngs west, overlying the Henty Adit andesites. In the west, south and north the sequence is truncated by the Henty Fault splay and the Howards Tramway Fault. The sequence comprises massive quartz feldspar crystal lithic sandstone, tuffaceous siltstones and calc-alkaline plagioclase pyroxene phyric lavas and dykes.

These andesites and those in the underlying Henty Adits sequence have been included in Suite I of the MRV by Crawford et al (1992). The Suite also includes the Que-Hellyer footwall andesites and Tyndall Group dacites and rhyolites.

Correlation of the Halls Rivulet Track Sequence with the Tyndall Group is based on the following points:

- andesite (No 30024B) is petrologically and geochemically very similar to that described by Pemberton et al (1991) (No 049) from the Cradle Mountain Link Road; this andesite occurring within Tyndall Group volcanics near the Denison Group contact.
- feldspar-quartz-crystal, lithic volcaniclastic sandstones are similar to those

in the Tyndall Group on the Anthony Road (Gibson, 1991).

The Ewart Creek Sequence is located in the western sector of fault wedge; comprising predominantly tholeiitic gabbros, dolerites and basaltic lavas interlayered with volcanoclastics very similar to those in the HRTS. Correlation of this sequence with the Tyndall Group is based on:

- volcanoclastics are dominated by feldspar-quartz-crystal sandstone with detrital magnetite and alternating chlorite albite alteration bands. This volcanoclastic is very similar to the Tyndall Group in the Queenstown area (Corbett, 1979), Anthony Road and Cradle Mountain Link Road (Gibson, 1991). It is recognised that similar albite chlorite alteration also occurs in the CVC (Eastoe et al, 1987) at a different stratigraphic level in the MRV, and hence the alteration style is not necessarily diagnostic of the Tyndall Group.
- Ewart Creek sequence immediately south of the study area is unconformably overlain by Denison Group siliciclastics (Baillie and Corbett, 1985), and in turn overlies the Yolande River Sequence (Fig 12). This association is very similar to that at Lynchford between the Yolande River Sequence - Tyndall Group - Denison Group (Corbett, 1979 and Dower, 1991).
- tholeiitic gabbros and basalts are comagmatic with the Henty Dyke Swarm (Corbett and McClenaghan 1985), the latter intruding CVC rhyolitic volcanics at White Spur, indicating a late Cambrian age for the tholeiites. Additional support for this Late Cambrian early Ordovician age tholeiitic magmatism has been reported by Pemberton et al (1991), describing tholeiitic lavas and intrusives in the Denison Group at Black Bluff Range and Tor Creek.

6.3.4 Ophiolite

A comparison of the HFW ophiolite with similar sized (6km²) Cambrian ultramafic complexes in western Tasmania, comprising cumulates, gabbro, tonalite and basalt-andesite lavas has been made and includes the McIvor Hill Complex and those at Cape Sorell (Timbertops and the Macquarie fault slices see Fig 1).

Most ultramafic complexes in western Tasmania are depleted in LREE and Zr (A.J. Crawford, pers. com., 1992) and their comagmatic lavas have depleted LREE or a characteristic basin shaped profile of the high magnesium andesites/boninites (Brown, 1986). Mafic rocks from the McIvor Hill Complex and Macquarie fault slices are in this group (Fig 15 and 16c).

A second ultramafic association can be recognised with relative LREE enrichment (Fig 16a and 16b) and higher Zr content for comparable SiO₂ levels (Fig 15). The HFW and possibly the Timbertops rocks comprise this group.

The McIvor Hill complex comprises a basal sliver of ultramafic overlain by gabbros and basaltic lavas; tonalites have intrusive contacts with the basalts (Olubas, 1989). REE patterns for tonalites show LREE depletion with a negative slope toward the LREE in chondrite normalized plots (Fig 16c). These trends are quite different to those of the HFW tonalites (Fig 16a) but have some similarities to gabbros from the fault bound ultramafics south of Macquarie Harbour (Fig 16c). These differences between the two gabbro-tonalite types can also be seen in the Zr-SiO₂ plot (Fig 15).

On the Macquarie 1:50000 sheet McClenaghan and Findlay (1989) have mapped two gabbro associations. The western gabbro is associated with

serpentinized ultramafics and tonalites in NNE trending fault zones (Macquarie fault slices). REE for this group are only available for gabbros and show a very depleted pattern with slight HREE enrichment (Fig 16c). Zr content is low ranging from 13ppm in gabbros to 46ppm in tonalites (Fig 15) and is similar to the McIvor Hill rocks.

The second gabbro association on the Macquarie sheet occurs at Timbertops where there is a spatial association between gabbro, andesite, felsic intrusives and talc altered mafics, the latter with relic spinels. The Timbertops association is interpreted as a plug like intrusive/volcanic complex with a common magma source. This comagmatic interpretation is supported by similar REE patterns from the different rock types (Fig 16b) reflecting a fractionation trend as defined by Cox et al (1979).

The Timbertops gabbro and tonalite can be readily differentiated from the Macquarie fault slice association to the west and McIvor Hill rocks on the basis of enriched LREE patterns (Fig 16b) and Zr content (Fig 15). From the REE plot the similarities between Timbertops and HFW mafic rocks can be seen (Fig 16a & b).

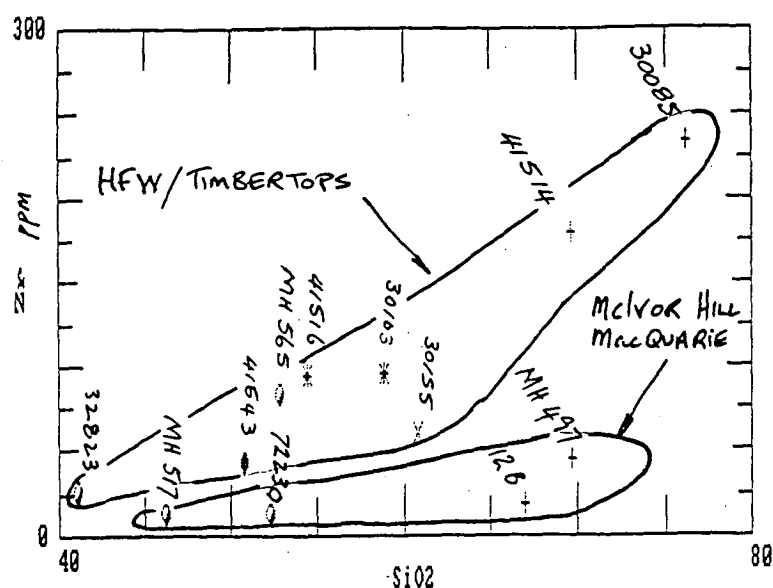
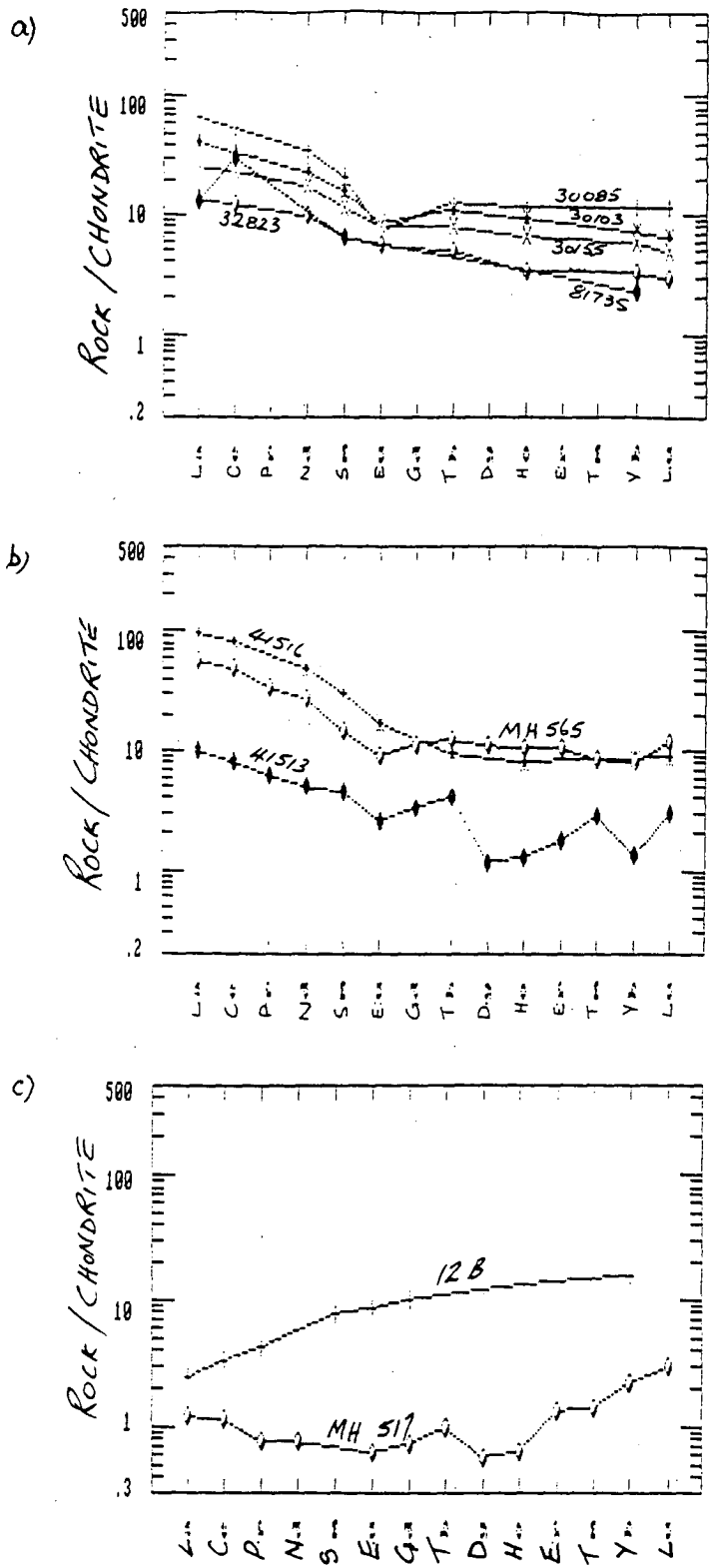


Figure 15 Zr - SiO₂ (mass %) plot, a comparison of two mafic - ultramafic associations in western Tasmania. Data is from the HFW (Table 2), from McClenaghan and Findlay 1989 (Table 5) and from Olubas 1989

Table 5 Rock descriptions and analytical data sources for samples plotted in Fig. 15b and c.

| SAMPLE | ROCK TYPE | LOCATION | DATA SOURCE |
|----------|------------|-------------|------------------------------|
| + MH 497 | Tonalite | Macquarie | McClenaghan and Findlay 1989 |
| ● MH 517 | Gabbro | " | " |
| ● MH 565 | Gabbro | Timbertops | " |
| + 41514 | Tonalite | " | " |
| * 41516 | Andesite | " | " |
| ● 41543 | Mafic lava | " | " |
| + 12B | Tonalite | McIvor Hill | Crawford pers com (1992) |
| ● 72230 | Gabbro | " | Olubas (1989) |



16. A comparison of chondrite-normalized REE patterns for mafic - ultramafic complexes in western Tasmania. For data sources and rock types see Table 4.

- a) Henty Fault Wedge
- b) Timbertops
- c) McIvor Hill and Macquarie

7. TECTONIC SETTING OF VOLCANICS AND INTRUSIVES

7.1 HENTY VALLEY SEQUENCE

On the basis of Ti Zr Nb REE geochemistry and lithological associations the basaltic andesites are similar to the CCF basalts. The CCF rocks have been interpreted by Crawford and Berry (1991) as continental tholeiites erupted onto an attenuated rifted passive continental margin. These rifts formed shallow basins (Haines 1991) and represent aborted rifts which failed to develop oceanic crust.

The presence of ultramafic and felsic volcanic detritus in the HVS greywackes indicates that the Henty Valley tholeiitic volcanism and sedimentation was either synchronous with or postdated the emplacement of ultramafics and eruption of felsic volcanics.

7.2 HENTY ADITS - HALLS RIVULET TRACK BASALTIC ANDESITE

The basaltic andesites have been included in Suite I of the MRV by Crawford et al (1992). These volcanics have compositional affinities with transitional medium to high K calc-alkaline orogenic andesites. However the occurrence of high K shoshonitic andesites in the MRV and boninitic lavas associated with ultramafics in the Dundas Trough (Crawford et al, 1992) indicate that there are significant differences between the MRV and orogenic andesites.

7.3 EWART CREEK SEQUENCE

This suite of tholeiitic basaltic lavas, dolerite and gabbroic intrusives are inter-layered with intermediate to felsic derived immature volcanoclastics. These tholeiites and the comagmatic Henty Dyke Swarm (Corbett and McClenaghan, 1985) form Suite IV of the MRV (Crawford et al, 1992) and are interpreted by them on the basis of chemistry as rift tholeiites. Nb values of <4ppm differentiate them from continental rift basalts which typically have values of >10ppm Nb (Pearce and Cann, 1973). On this basis Crawford et al (1992) consider that the basalts were emplaced in a supra subduction regime associated with the early phase of back arc basin opening in the late Cambrian and towards the end of MRV volcanism.

7.4 OPHIOLITE

The ultramafic complex in the HFW has similarities to the ophiolite layers described by Nicolas (1989), which from the base upward include serpentized foliated cumulates, sheeted dyke complex and lavas. Three tectonic settings for ophiolites have been described by Nicholas (1989); these settings include mid oceanic ridge, island arc and back arc basin.

Features associated with the HFW ophiolite which give an indication of the tectonic environment of formation include:

- a sedimentary top which has a significant terrigenous component derived from continental basement.
- lavas and some dykes are andesitic and have calc-alkaline affinities (Fig 7).
- gabbro and andesitic dyke swarms indicate an extensional environment.

- tonalites are LREE enriched, consistent with Arth's (1979) findings that these enriched tonalites are associated with continental crust.

On the basis of the above features the interpreted setting of HFW ophiolite complex is a back arc basin developed within or adjacent to Precambrian continental basement.

The basin was probably located in the western part of the Dundas Trough, and possibly contemporaneous with the mid to late Cambrian MRV. A modern analogue is the Sea of Japan in which two areas of oceanic crust are separated by the continental crust of the Yamoto Rise (Tamaki, 1985 in Cas and Wright, 1987).

Ultramafic cumulates and associated volcanics at McIvor Hill (Olubas, 1989) and Serpentine Hill (Brown, 1986 and Crawford and Berry, 1991) are interpreted as obducted slices of the fore arc region of an oceanic island arc, with a modern analogue the West Pacific island arc (Crawford and Berry, 1991).

The occurrence of two ultramafic associations ie HFW type and McIvor Hill type within the Dundas Trough is the result of thrust stacking of island arc and back arc basin complexes during collision. The two associations forming in different tectonic regimes associated with an active continental margin.

Similar juxtaposition of different ultramafic terrains has been described by Malpas (1979) in Newfoundland where oceanic and island arc complexes have been juxtaposed by thrust stacking.

8. STRUCTURAL GEOLOGY

8.1 Introduction

The HFW is bounded by the SHF in the east, NHF in the west and is overlapped by Cambro-Ordovician cover in the south. Sequences within the wedge, including the ophiolite strike N to NNW, dip moderately to steeply west and young to the west. Folds, where observed are broad open structures; exceptions occur in the structurally complex zone between the SHF splays at the Henty Valley Prospect.

Cleavage is well developed in finer grained sediments and is predominantly WNW trending, at right angles to the compression transport direction defined by Keele (1991) in his domains 10 and 11. Significant deviation from this regional cleavage trend occurs within the fault zones and particularly at the Henty Valley Prospect between the SHF splays where east-west trends are developed. This east-west trend is coincident with a regional corridor of anomalous aeromagnetic responses (Leaman, 1991).

On the basis of structural domain mapping, Keele (1991) has subdivided the fault wedge into two domains (Fig 17). Sediments and volcanics NE of the Howards Tramway Fault are included in domain 11, and the ophiolite and Ewart Creek Sequence to the SW in domain 10. Additional domains may exist; these include the hematitic siltstone in the apex of HFW north of the White Spur Creek Fault and the Henty Valley wedge between splays of the SHF.

metres wide (eg 57900N) or a zone up to 200m wide of shearing, incorporating slivers of lithologies from both the footwall and hanging wall of the fault (eg 53000N and 60000N).

Pervasive sericite-carbonate-pyrite alteration occurs along the entire strike length of the structure, with the best exposure and development in felsic volcanics in the Hydro Electric Commission's Henty Canal at 61000N.

Interpreted movement on the fault includes significant dip and strike slip components, juxtaposing unlike sequences and truncating magnetic trends (Fig 3). A dextral strike slip movement is the dominant interpreted displacement on the structure. On a local scale this dextral motion is based on the displacement of HAS andesite lavas between the Henty Valley and Henty Adits Prospects, and on a regional scale the emplacement of Crimson Creek Formation, Dundas Group, Tyndall Group and ophiolite into the CVC.

8.3 NORTH HENTY FAULT

This fault forms the contact between the HFW and the CVC and overlying White Spur Formation to the west.

Unlike the SHF, the structure is not a prominent feature topographically; the only exposure is located at the junction of the Henty River and White Spur Creek.

South of the junction with the WSCF, the structure is associated with altered ultramafic slivers <100m thick. The ultramafics are fault bound and not related to hanging wall or foot wall lithologies except at the intersection with the Howards Tramway Fault.

A moderate west dip to the structure is based on aeromagnetics (Fig 3) and 2D magnetic modelling (Leaman, 1991). The prominent magnetic anomaly associated with the ultramafics (0.01-0.03cgs) can be seen extending beneath the White Spurt Formation (0.0002cgs) in Fig 3.

8.4 HOWARDS TRAMWAY FAULT

This is a north-south trending structure which coalesces with the SHF at 5330000N and intercepts the NHF at 5357000N, displacing this latter structure by 1km of sinistral movement (Fig 2).

The fault is associated with serpentinized ultramafics at the base of the ophiolite and is best exposed in road cuttings on the Halls Rivulet track.

Based on magnetic modelling, the structure has a vertical dip (Leaman, 1991). Significant reverse movement is interpreted, oceanic like crust of the ophiolite being juxtaposed with Tyndall Group volcanoclastics to the east.

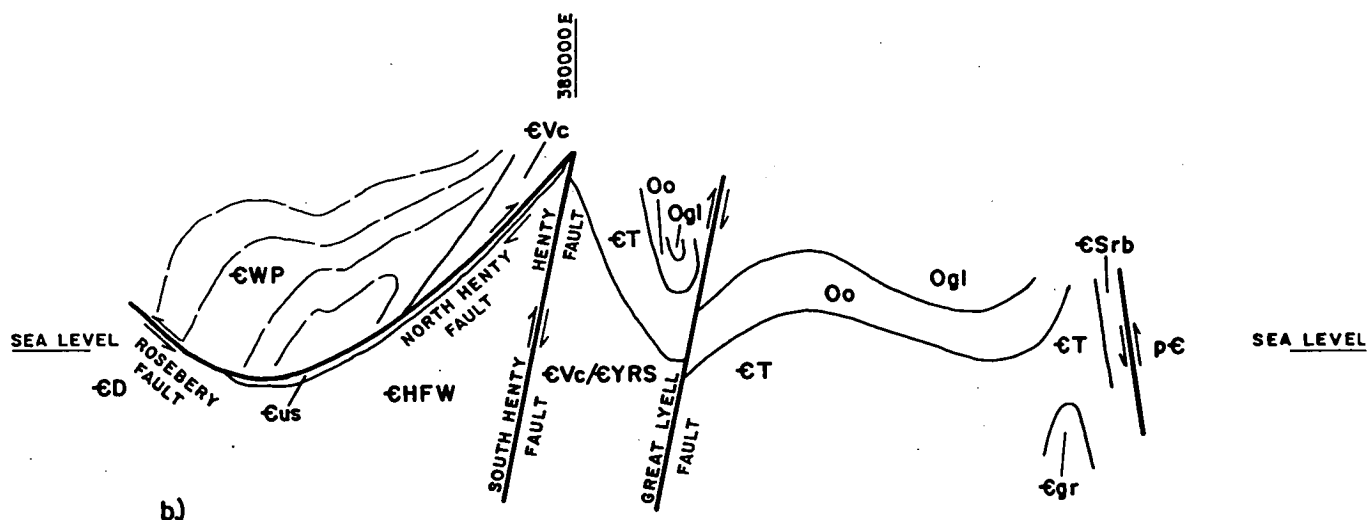
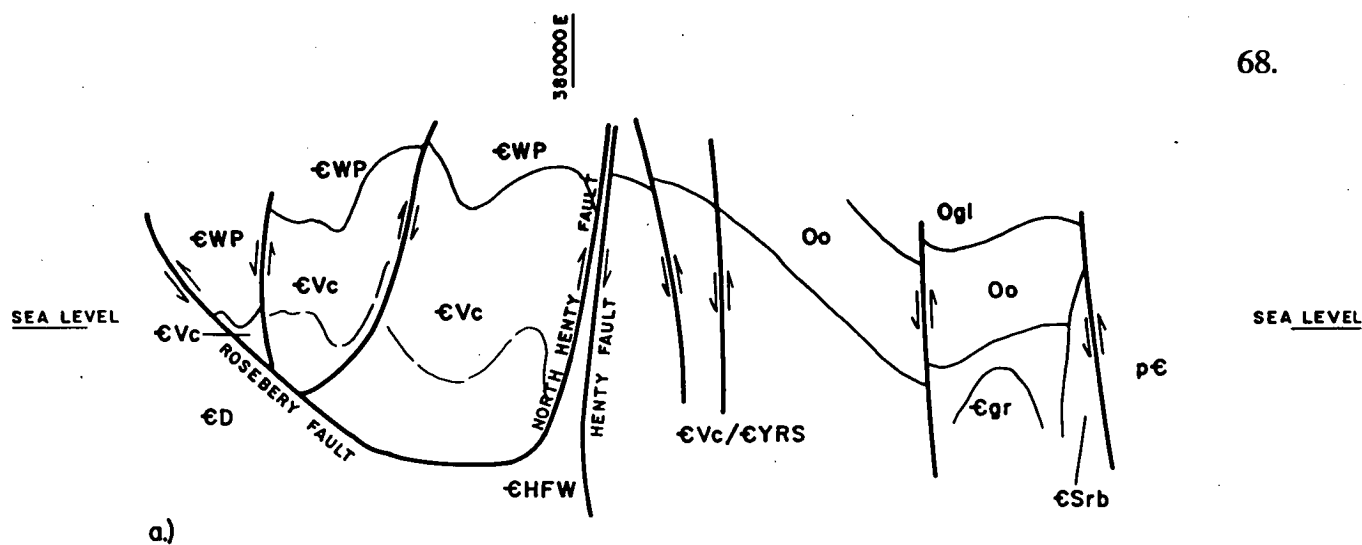
8.5 RELATIONSHIP BETWEEN FAULTS/FAULT MOVEMENTS

The SHF and HF are considered to be one and the same continuous primary structure based on their similar strike and dip. Significant dextral strike slip movement is interpreted with transport from the SW. The structure is steep, rooted in basement and has been a focus for tholeiitic Henty Dyke Swarm magmatism.

The poor definition of the fault in outcrop south of 5350000N may indicate that the structure was inactive in this area in the late Cambrian and has been obscured by Cambro-Ordovician cover rocks (Fig 13).

The Rosebery Fault (RF) is an east dipping thrust located 5km west of the NHF, its location and attitude has been well constrained by drilling (Corbett and Lees, 1987). Both the RF and NHF have been interpreted to be associated with Devonian D1 compression (Keele, 1991). The faults are interpreted to form the thrust sole to a positive flower or pop up structure of CVC and overlying WSF (Fig 18). Footwall to this structure, shortening has been taken up by folding and thrusting in the HFW - Dundas Group volcanics, sediments and ultramafics. This association between the two thrusts may extend north to the Pinnacles - Mackintosh Dam area at 5385000N. The Farrel Slates at Tullah may equate with the HFW sediments (Keele, 1991), bound by the west dipping NHF thrust to west and the HF to the east.

Implications of this interpretation are that the combined north plunging NHF and RF thrust plane would outcrop at about 5356000N in the Howards Road area; south of this point all exposures are below the thrust surface. Secondly to some extent the CVC between White Spur and Pinnacles - Mackintosh are rootless or in some degree displaced from their subvolcanic counterparts, an argument forwarded by Leeman (1991) based on gravity features associated with primary rift edges of the Tyennan Block in the Rosebery area. A third point is that unlike the HF/SHF the thrust is a surficial structure, obscuring lithologies of the HFW rather than forming the western margin to a fault wedge (Fig 18b).



a.) 66500 N Rosebery Mine Lease. Modified after Fig.5 Keele, 1991.

b.) 58500 N E.L. 11/85 YOLANDE (HENTY).

LEGEND

| | | | | |
|--------------|------|----------------------|------|------------------------|
| Ordovician - | Ogl | Gordon Limestone | €Vc | Central Volcanics |
| | Oo | Owen Conglomerate | €D | Dundas Group |
| Cambrian - | €T | Tyndall Group | €HFW | Henty Fault Wedge |
| | €gr | Murchison Granite | €YRS | Yolande River Sequence |
| | €Srb | Sticht Range Beds | €us | Ultramafics |
| | €WP | White Spur Formation | p€ | Pre Cambrian |



PASMINCO EXPLORATION

A Division of Pasminco Australia Limited

COMPILED: R.A.P.

DATE: 18-7-92

DRAWN: N.W.D.S.

REF.:

REVISIONS:

DRAWING No.

INTERPRETIVE GEOLOGICAL
SECTIONS, SHOWING
RELATIONSHIPS BETWEEN
MAJOR FAULTS

SCALE 1:100,000 0 1 2km.

PAS. No.
18

9. CONCLUSIONS

Stratigraphy preserved in the HFW represents a Cambrian section from the basal eo-Cambrian Crimson Creek Formation to the late Cambrian Tyndall Group. Two sequences, eastern and western, are recognized, the two divided by the Howards Tramway Fault.

The Henty Valley Sequence, the base of the eastern sequence, comprising tholeiitic basalts, cherts and hematitic wackes has geochemical and lithological similarities to both the eo-Cambrian Crimson Creek Formation and mid Cambrian Dundas Group. This apparent contradiction is resolved if the sequence is considered as a distal basin, spanning events from early Cambrian rift magmatism through ultramafic obduction to mid Cambrian Mt Read volcanism.

The Henty Adits and Halls Rivulet Track sequence overlies the Henty Valley sequence and includes calc-alkaline MRV andesites and is interpreted to represent a transition from mid Cambrian Dundas Group to late Cambrian Tyndall Group volcanism.

The western sequences comprise an ultramafic complex and the Ewart Creek tholeiite lavas and intrusives.

The ultramafic is REE and Zr enriched, and has calc-alkaline affinities with similarities to the Timbertops intrusives south of Macquarie Harbour. Geochemically these complexes are unlike the majority of ultramafics in western Tasmania. The HFW complex is interpreted to represent an extensional tectonic regime in which oceanic like crust was formed in a back arc basin environment associated with the Mt Read Volcanics.

The Ewart Creek package unconformably overlies or is faulted against the ultramafic, and in turn is unconformably overlain by basal Ordovician sediments. Tholeiitic intrusives and extrusives are comagmatic with the late Cambrian Henty Dyke Swarm. On the basis of tholeiites, volcanoclastic type and relationship with basal Ordovician, the sequence is correlated with the Tyndall Group.

Bounding structures of the fault wedge are the SHF and NHF. The SHF and HF are interpreted as the same structure, a steep dipping fault that is rooted in basement and has been a focus for tholeiitic magmatism. Movement is interpreted as mainly dextral strike slip with some reverse component, bringing the Crimson Creek Formation and distal facies of the Dundas Group into juxtaposition with proximal MRV facies.

The HF/SHF was active through most of the Cambrian and forms a fundamental break in the MRV. Late Cambrian Ewart Creek and Denison Group cover sequences on lap the fault in the SW placing a limit of late Cambrian age on the fault movement in this area.

In contrast the NHF is considered a surficial, Devonian age structure which has acted in unison with the RF to the west. These two moderate dipping thrusts form the sole of a positive flower/pop up structure which plunges north.

The implications of this combined RF NHF thrust plane is that the MRV CVC north of Howards Road may be rootless and the HFW is only an apparent wedge. The lithologies of the HFW continuing west beneath the CVC and are part of the same structural block as Dundas to the west.

REFERENCES

- Adachi, A., Yamamoto, K., and Sugisaki, R., 1986 Hydrothermal chert and associated siliceous rocks from the northern Pacific: Their geological significance as indication of ocean ridge activity. *Sedimentary Geology* Vol. 47, p.125-148.
- Arculus, R.J., 1987 The significance of source versus process in the tectonic controls of magma genesis, *Journ. Volcanol. Geotherm. Res.*, 32, 1-12.
- Arth, J.G., 1979 Some trace elements in trondhjemites - their implications to magma genesis and palaeotectonic setting. In: Barker, F. (Ed) *Development in petrology 6. Trondhjemites, dacites and related rocks.* Elsevier Scientific Pub. Co.
- Baillie, P.W., and Corbett, K.D., 1985 Strahan, Geological Surv. Explan. Rept: Tas. Dept. Mines, Geol Atlas 1:50,000 Series Sheet 57 (7913N).
- Barker, F., 1979 *Developments in petrology 6. Trondhjemites, dacites and related rocks.* Elsevier Scientific Pub Co.
- Barker, F., 1979 Trondhjemite: Definition, Environment and Hypotheses of origin. In: Barker, F. (Ed) *Developments in petrology 6. Trondhjemites, dacites and related rocks.* Elsevier Scientific Pub. Co.
- Barwick, D.C., 1991 Geology and mineralization of the Sock Creek and High Point areas, Western Tasmania: B.S.C. (Hons) thesis (unpub.), Univ. of Tasmania.
- Berry, R.F., 1989 The history of movement on the Henty Fault zone, western Tasmania: an analysis of fault striations. *Australian Journal of Earth Sciences* 36, 189-206.
- Berry, R.F., 1991 An excursion guide for the Mt Lyell Mining Lease with emphasis on the Great Lyell Fault, Haulage Unconformity and North Lyell alteration. In: *Structure and mineralization of western Tasmania, AMIRA Project P.291 Report No. 2, CODES Univ. of Tasmania.*
- Brown, A.V., 1986 Geology of the Dundas - Mount Lindsay - Mount Youngbuck Region. *Geol. Surv. Tasmania Bull.* 62.

Burrett, C.F. and Martin, E.L., 1989 (Eds.) *The Geology of Tasmania: Geol. Soc. Aust. Spec. Publ. 15.*

BVSP 1981 *Basaltic Volcanism on the Terrestrial Planets.* Pergamon Press, New York.

Cas, R.A.F. and Wright, J.V., 1987 *Volcanic Successions Modern and ancient - A geological approach to processes, products and successions.* Unwin Hyman, London.

Corbett, K.D., 1979 *Stratigraphy, correlation and evolution of the Mt Read Volcanics in the Queenstown, Jukes - Darwin and Mt Sedgwick areas: Tasmania Dept. of Mines: Geological Survey Bulletin 58.*

Corbett, K.D., 1985 *The Bradshaws Road drill hole through the South Henty Fault Zone, western Tasmania: Tas. Dept. of Mines Unpub. Report 1985/56.*

Corbett, K.D., 1989 *Stratigraphy, Palaeogeography and Geochemistry of the Mt Read Volcanics.* In: Burrett, C.F. and Martin, E.L., (Eds.) *The Geology of Tasmania: Geol. Soc. Aust. Spec. Publ. 15.*

Corbett, K.D., and Komyshan, P., 1989 *Geology of the Hellyer - Mt. Charter area: Mt Read Volcanics Project Geological Report 1 Tas. Dept. Mines.*

Corbett, K.D., and Lees, T.C., 1987 *Stratigraphic and structural relationships and evidence for Cambrian deformation at the western margin of the Mt Read Volcanics, Tasmania: Australian Jour. Earth Sci., v. 34.*

Corbett, K.D., and McClenaghan, M.P. 1985 *Geochemical diagrams of Cambrian rocks and associated intrusions from western Tasmania: Tas. Dept. Mines Unpubl. Rept. 1985/63.*

Cox, K.G., Bell, J.D., and Pankhurst, R.J., 1979 *The interpretation of igneous rocks.* Pub. Allen and Unwin.

Crawford, A.J., 1989 *The petrology, geochemistry and tectonic significance of igneous rocks in the Henty Fault Wedge, western Tasmania: A report for Pasminco Mining, Rosebery, Tasmania: In: E.L. 11/85 Yolande J.V., Annual Report to 20th July, 1990.*

Crawford, A.J. and Berry, R.F., 1991 Tectonic implications of Late Proterozoic - Early Palaeozoic igneous rock associations in western Tasmania: Tectonophysics in press.

Crawford, A.J., 1990 Petrographic reports, Rocks from Pasminco EL 11/85 Yolande. Appendix D In: Poltock and FitzGerald, Annual report for 12 months to July 1991 and Appendix G In: Poltock, Annual Report for 12 months to July 1992.

Crawford, A.J., Corbett, K.D., and Everard, J.L., 1992 Geochemistry of the Cambrian VHMS-Rich Mount Read Volcanics, Tasmania, and some tectonic implications Econ. Geol. Vol. 87 (3).

Date, J., Watanabe, Y., and Saeki, Y., 1983 Zonal alteration around the Fukazawa Kuroko deposits, Akita Prefecture, northern Japan. Econ. Geol. Monogr. 5, 365-386.

Dower, B.J., 1991 The geology, geochemistry and tectonic setting of the Miners Ridge Basalt and Lynch Creek Basalt in the Mount Read Volcanic Belt, western Tasmania: B.Sc. (Hons) thesis (unpub.), Univ. of Tasmania.

Eastoe, C.J., Solomon, M., and Walsh, J.L., 1987 District scale alteration zoning associated with massive sulfide mineralization in the Mt Read Volcanics, western Tasmania. Econ. Geol. 82(5): 1239-1258.

Finlow-Bates, T. and Stumpfl, E.F., 1981 The behaviour of so called immobile elements in hydrothermally altered rocks associated with volcanogenic submarine-exhalative ore deposits. Mineral. Deposita. 16, 319-328.

Floyd, P.A., and Winchester, J.A., 1975 Magma type and tectonic setting discrimination using immobile elements. Earth and Planetary Science Letters, 27 (1975) 211-218.

Gibson, R.P., 1991 The geology of the Mount Read Volcanics in the Anthony Road - Newton Creek area, Western Tasmania. Honours Thesis Geology Dept. Univ. Tas.

Glennie, K.W., 1970 Desert sedimentary environments: In: Developments in sedimentology No. 14.

Green, G.R., 1990 Alteration mineralogy, whole rock geochemistry and oxygen isotope zonation in the area north of the Grand Centre Prospect, Rosebery Mine Leases: A report for Pasminco Mining Rosebery: Mines consultancy services: Tas. Mines Dept. Unpub. Rept.

Greensmith, J.T., 1989 Petrology of sedimentary rocks Unwin and Hyman, London: Page 153-163.

Haines, J.B., 1991 The stratigraphy and sedimentology of the lower Crimson Creek Formation and related mafic igneous rocks, Renison Bell Mine: B.Sc. (Hons) thesis (unpub.), Univ. of Tasmania.

Hesse, R., 1988 Diagenesis #13. Origin of chert: Diagenesis of biogenic siliceous sediments. Geoscience Canada Vol. 15 No. 3.

Iijima, A., Hein, J.R., and Siever, R., (Eds.) Siliceous deposits in the Pacific region. Developments in sedimentology 36.

Imoto, N., 1983 Sedimentary structures of Permian-Triassic Cherts in the Tamba District, Southwest Japan. In: Iijima, A., Hein, J.R., and Siever, R., (Eds.) Siliceous deposits in the Pacific region. Developments in sedimentology 36.

Irvine, T.N., and Baragar, W.R.A., 1971 A guide to the chemical classification of the common volcanic rocks. Can. J. Earth Sci. 8:523-548.

Jenkins, G.W., 1990 EL 11/85 Yolande J.V., Annual Report to 20th July, 1990 Pasminco Mining Rosebery.

Joyce, A.S., 1987 Petrological report on twelve samples from E.L. 11/85 on the Henty Fault Zone, Tasmania: Appendix iii In: Poltock 1987, EL 11/85 Newton Creek - Gold potential of the North and South Henty Faults, May - August 1987.

Keele, R.A., 1991 The Zeehan - Red Hills - Lake Selina Traverse - A domain approach to the analysis of structural data. CODES: AMIRA Project P.291 - Structure and mineralisation of western Tasmania. November 1991.

Leaman, D.E., 1991 EL 11/85: Yolande River (Henty) Interpretation update for Pasminco Exploration In: Poltock 1992, Annual Report EL 11/85 Yolande.

Leaman, D.E., 1992 Yolande River EL 11/85, Comments on implications of new gravity data (Interim notes) In: Poltock 1991, Annual Report EL 11/85 Yolande.

Malpas, J., 1979 Two contrasting trondhjemite associations from transported ophiolites in western Newfoundland: initial report. In: Barker, F. (Ed) Developments in petrology 6. Trondhjemites, dacites and related rocks. Elsevier Scientific Pub. Co.

McClenaghan, M.P., 1989 Mid-Palaeozoic granitoids In: C.F. Burrett and E.F. Martin (Eds.) The Geology of Tasmania Geol. Soc. Aust. Spec. Publ. 15.

McClenaghan, M.P., and Findlay, R.H. 1989 Macquarie Harbour, Tasmania. Tas. Dept. Mines, Geol. Atlas 1:50,000 Series Sheet 7913S (64).

Meares, R.M.D., 1980 Geology, mineralization and alteration of the Southern Henty Gorge Lead-Zinc Prospect, western Tasmania MSc. thesis James Cook University of North Queensland (Unpub.).

Miyashiro, A., 1974 Volcanic rock series in island arcs and active continental margins. American Journ. of Sci., Vol. 274 p.321-355.

Nicolas, A., 1989 Structure of ophiolites and dynamics of oceanic lithosphere. Dordrecht: Kluwer Academic Publishers.

Norrish, K., and Chappell, B.W., 1967 X-ray fluorescence spectrography. In: Zussman, J. (Ed.). Physical methods in determinative mineralogy. Academic Press London.

Olubus, P.E., 1989 The geology of the McIvor Hill Complex. B.Sc. (Hons) thesis (unpub.), Univ. of Tasmania.

Pearce, J.A., and Cann, J.R., 1973 Tectonic setting of basic volcanic rocks determined using trace element analysis: Earth and Planetary Sci. Let. 19 (1973) 290-300.

Pemberton, J., Vicary, M.J., and Corbett, K.D., 1991 Geology of the Cradle Mountain Link Road - Mt Tor area. Tas. Dept. of Resources and Energy: Mt Read Volcanics Project Geological Report 4.

Poltock, R.A., 1987 EL 11/85 Yolande - Newton Creek. Gold potential of the North and South Henty Faults.

Poltock, R.A., 1992 Annual report EL 11/85 Yolande. Pasminco Exploration.

Poltock, R.A. and FitzGerald, F.G., 1991 Annual report EL 11/85 Yolande. Pasminco Exploration.

Saito, Y., Tiba, T., and Matsubara, S., 1988 Precambrian and Cambrian Cherts in north western Tasmania: Bull. Nat. Sci. Mus., Tokyo, Ser. C., 14 (2), pp.59-70.

Stolz, J., and Large, R.R., 1992 Evaluation of the Source-Rock Control on Precious Metal Grades in Volcanic-Hosted Massive Sulfide Deposits from Western Tasmania. Econ. Geol. Vol. 87(3).

Taylor, B.L., 1954 Progress report on the North Pieman mineral area. Unpub. Rep. Dept. Mines Tas. 1954:149-203.

Williams, E., McClenaghan, M.P., and Collins, P.L.F. 1989 Mid-Palaeozoic Deformation, Granitoids and Ore Deposits. In: Burrett, C.F. and Martin, E.L. (Eds.) The Geology of Tasmania. Geol. Soc. Aust. Spec. Publ. 15.

Wilson, M., 1989 Igneous petrogenesis - A global tectonic approach. Unwin Hyman.

APPENDICES

APPENDIX 1.

HENTY FAULT WEDGE SAMPLE CATALOGUE.

| SAMPLE | N | E | TS | MT | REE | PROBE |
|--------|--------|-------|----|----|-----|-------|
| 30002 | 55600 | 76360 | x | | | |
| 30003 | 55600 | 76040 | x | | | |
| 30024A | 55246 | 77115 | x | | | |
| 30024B | 55246 | 77115 | x | x | x | |
| 30054 | 52140 | 73350 | x | | | |
| 30055 | 52157 | 73350 | x | x | | |
| 30057 | 52200 | 74570 | x | | | |
| 30061 | 51600 | 74100 | x | | | |
| 30078 | 52400 | 74500 | x | | | |
| 30081 | 52400 | 75060 | x | | | |
| 30085 | 52190 | 75450 | x | x | x | |
| 30087 | 52000 | 75705 | x | | | |
| 30091 | 51800 | 75160 | x | | | x |
| 30099 | 53200 | 76590 | x | x | | |
| 30102 | 53195 | 74946 | x | x | | |
| 30103 | 53198 | 74870 | x | x | x | |
| 30105 | 53605 | 74320 | x | x | | |
| 30106 | 53600 | 74680 | x | | | |
| 30117 | 52794 | 76080 | x | x | | |
| 30124 | 54013 | 74548 | x | x | | |
| 30126 | 54394 | 74780 | x | x | | |
| 30136 | 55600 | 78020 | x | | | |
| 30141A | 55300 | 77400 | x | | | |
| 30141B | 55300 | 77400 | x | | | |
| 30155 | 54789 | 75861 | x | x | x | |
| 30156 | 54800 | 75800 | x | | | |
| 30159 | 54791 | 75720 | x | x | | |
| 30173 | 51197 | 75069 | x | x | x | |
| 30175 | 51200 | 75350 | x | x | | |
| 30179 | 51000 | 75250 | x | | | |
| 30194 | 51195 | 73588 | x | x | | |
| 30857 | DD HR5 | 102m | x | x | x | |
| 30862 | DD HR5 | 156m | x | x | | |
| 30866 | DD HR5 | 192m | x | | | |
| 30869 | DD HR5 | 231m | x | x | | |
| 30872 | DD HR5 | 272m | x | | | |
| 30875 | DD HR5 | 305m | x | | | |
| 30881 | DD HR5 | 322m | x | | | |
| 30889 | DD HR5 | 337m | x | x | x | |
| 30913 | 56425 | 76700 | x | | | |
| 30922 | 56730 | 76310 | x | x | | |
| 30963 | 53375 | 74200 | x | | | |
| 30971 | 52300 | 74950 | x | | | |
| 30973 | 59880 | 78890 | x | x | | |
| 30980 | 59750 | 78838 | x | x | x | |
| 30982 | 55300 | 76900 | x | | | |
| 30986 | 51075 | 74100 | x | | | |
| 30987 | 51089 | 74094 | x | x | x | |
| 30989 | 51230 | 75125 | x | | | x |
| 31507 | 57470 | 77440 | x | | | |
| 31580 | 58910 | 78525 | x | | | |
| 31606 | 56640 | 77400 | x | | | |

| | | | | | |
|--------|--------|--------|---|---|---|
| 31607 | 56675 | 77440 | x | | |
| 31641 | 51285 | 75328 | x | x | x |
| 31648 | 51345 | 75360 | x | | |
| 31651B | 51345 | 75360 | x | | |
| 31653 | 50275 | 74250 | x | | |
| 31664 | 51555 | 75260 | x | | |
| 31666 | 51524 | 75358 | x | x | |
| 31676 | 51476 | 75256 | x | x | |
| 31678 | 51600 | 75700 | x | | |
| 31683 | 50962 | 75126 | x | x | |
| 31688 | 50850 | 75060 | x | | |
| 31700 | 50600 | 75210 | x | | |
| 32102 | DD BR1 | 80.5m | x | | |
| 32103 | DD BR1 | 84.3m | x | | |
| 32104 | DD BR1 | 340.6m | x | | |
| 32105 | DD BR1 | 470.2m | x | | |
| 32153 | 58360 | 79150 | x | | x |
| 32170 | 58535 | 79039 | x | x | x |
| 32176 | 59200 | 79300 | x | | |
| 32188 | 57600 | 79200 | x | | |
| 32197 | 59595 | 78779 | x | x | x |
| 32806 | 60032 | 78770 | x | x | |
| 32823 | 56310 | 76030 | x | x | |
| 32838 | 51300 | 75250 | | x | |
| 32839 | 51290 | 75290 | | x | |
| 32841 | 51260 | 75350 | | x | |
| 32842 | 51250 | 75400 | | x | |
| 32844 | DD HR3 | 301.7m | | x | |
| 32845 | DD HR3 | 302.0m | | x | |
| 32846 | DD HR3 | 322.5m | | x | |
| 216466 | 59025 | 78980 | x | | |
| 216511 | 59900 | 78525 | x | | |
| 216512 | 59900 | 78525 | x | | |
| 216515 | 59850 | 78880 | x | | |
| 216519 | 57750 | 78500 | x | | |
| 216522 | 57650 | 79040 | x | | |
| 216525 | 57650 | 79040 | x | | |

Coordinates AMG

TS - thin section

MT - major and trace element analyses

REE - rare earth element analyses

Probe - electron microprobe

APPENDIX 2.

MAJOR, TRACE AND RARE EARTH ELEMENT ANALYSES FOR HENTY FAULT
WEDGE IGNEOUS ROCKS.

| Sample | 300248 | 30055 | 30085 | 30099 | 30102 | 30103 | 30105 | 30117 | 30124 | 30126 |
|--------------------------------|---------|---------|---------|---------|---------|---------|---------|---------|---------|---------|
| Noting | 5355246 | 5352157 | 5352190 | 5353200 | 5353195 | 5353198 | 5353605 | 5352744 | 5354013 | 5354394 |
| Easting | 377115 | 375470 | 375450 | 376890 | 376946 | 376875 | 374320 | 376080 | 374348 | 374780 |
| Symbol | 8 | 14 | 13 | 9 | 11 | 11 | 14 | 13 | 14 | 11 |
| Sym Colour | - | 1 | 1 | 1 | 1 | 1 | 1 | 1 | 1 | 1 |
| Rock Type | ELbn1 | EL/Ib | EIt | CVr | EVn1 | EVn1 | EL/Ib | EIt | EL/Ib | EL/Ib |
| SiO ₂ | 60.94 | 52.48 | 76.16 | 66.70 | 62.35 | 58.90 | 52.10 | 63.87 | 51.34 | 37.35 |
| TiO ₂ | 0.72 | 0.76 | 0.45 | 0.70 | 0.49 | 0.51 | 0.82 | 0.53 | 0.76 | 0.46 |
| Al ₂ O ₃ | 14.58 | 19.10 | 12.30 | 14.00 | 17.87 | 17.39 | 19.58 | 17.56 | 16.85 | 16.27 |
| Fe ₂ O ₃ | 7.01 | 8.95 | 4.89 | 4.72 | 6.36 | 6.95 | 7.65 | 7.90 | 9.10 | 6.23 |
| FeO | - | - | - | - | - | - | - | - | - | - |
| MnO | 0.16 | 0.15 | 0.03 | 0.11 | 0.09 | 0.12 | 0.12 | 0.10 | 0.37 | 0.14 |
| MgO | 4.73 | 5.88 | 2.37 | 1.46 | 3.92 | 8.71 | 5.11 | 5.58 | 4.09 | 8.50 |
| CaO | 5.77 | 5.62 | 0.10 | 2.03 | 0.25 | 2.28 | 5.62 | 0.21 | 11.67 | 4.44 |
| Na ₂ O | 3.82 | 4.87 | 2.58 | 1.60 | 8.48 | 3.63 | 4.03 | 2.40 | 3.58 | 5.92 |
| K ₂ O | 2.12 | 2.06 | 1.06 | 3.03 | 0.11 | 1.42 | 0.84 | 1.74 | 1.94 | 0.63 |
| P ₂ O ₅ | 0.14 | 0.15 | 0.06 | 0.10 | 0.08 | 0.09 | 0.13 | 0.04 | 0.12 | 0.07 |
| Total | 99.99 | 99.56 | 100.00 | 94.45 | 100.01 | 100.00 | 100.00 | 100.00 | 100.00 | 100.02 |
| Mg # | 57.20 | 36.46 | 46.88 | 37.99 | 34.67 | 71.28 | 56.95 | 58.31 | 47.08 | 72.99 |
| Cr | 136 | 34 | 7 | - | 134 | 402 | 123 | 79 | 25 | 351 |
| Ni | 38 | 38 | 15 | - | 78 | 269 | 66 | 45 | 39 | 186 |
| V | 180 | 241 | 40 | - | 43 | 108 | 179 | 141 | 238 | 109 |
| Cu | 3 | 196 | 210 | - | 4 | 17 | 103 | 8 | 11 | 7 |
| Pb | 16 | 8 | 3 | - | 10 | 7 | 7 | 4 | 6 | 5 |
| Zn | 111 | 92 | 37 | - | 58 | 72 | 65 | 98 | 184 | 70 |
| K | 17598 | 17100 | 6799 | 25152 | 913 | 11787 | 6973 | 14444 | 16104 | 5236 |
| Rb | 67 | 57 | 30 | 160 | 2 | 35 | 25 | 55 | 81 | 13 |
| Sr | 338 | 596 | 31 | 45 | 56 | 183 | 281 | 31 | 137 | 255 |
| Na | 12.5 | 1.9 | 13.2 | - | 8.0 | 8.9 | 2.7 | 9.1 | 4.4 | 8.1 |
| Ir | 185 | 69 | 234 | 260 | 97 | 96 | 72 | 113 | 62 | 95 |
| Ti | 4316 | 4556 | 2698 | 4197 | 2938 | 3057 | 4916 | 3537 | 4556 | 2758 |
| Y | 29 | 28 | 25 | 30 | 18 | 19 | 24 | 13 | 25 | 23 |
| Th | 13.00 | 8.00 | 11.00 | - | 6.00 | 6.00 | 5.00 | 8.00 | 6.00 | 7.00 |
| La | 28.10 | - | 21.60 | - | - | 13.60 | - | - | - | - |
| Ce | 60.80 | - | 46.90 | - | - | 28.60 | - | - | - | - |
| Pr | - | - | - | - | - | - | - | - | - | - |
| Nd | 28.50 | - | 22.40 | - | - | 15.00 | - | - | - | - |
| Sm | 5.94 | - | 4.17 | - | - | 3.30 | - | - | - | - |
| Eu | 1.32 | - | 0.57 | - | - | 0.67 | - | - | - | - |
| Gd | - | - | - | - | - | - | - | - | - | - |
| Tb | 0.96 | - | 0.65 | - | - | 0.56 | - | - | - | - |
| Dy | - | - | - | - | - | - | - | - | - | - |
| Ho | 1.13 | - | 0.91 | - | - | 0.72 | - | - | - | - |
| Er | - | - | - | - | - | - | - | - | - | - |
| Yb | 2.60 | - | 2.55 | - | - | 1.59 | - | - | - | - |
| Lu | 0.39 | - | 0.40 | - | - | 0.22 | - | - | - | - |
| Density | 2.56 | 2.56 | 2.58 | 2.40 | 2.44 | 2.52 | 2.58 | 2.48 | 2.60 | 2.52 |

| Sample | 30153 | 30159 | 30173 | 30194 | 30857 | 30862 | 30869 | 30889 | 30922 | 30973 |
|--------------------------------|---------|---------|---------|---------|-------|--------|-------|--------|---------|---------|
| Northing | 5354789 | 5354791 | 5355197 | 5355195 | HR 5 | HR 5 | HR 5 | HR 5 | 5356730 | 5359880 |
| Easting | 375861 | 375720 | 375069 | 375799 | 102m | 156m | 231m | 337m | 376310 | 378890 |
| Symbol | 12 | 12 | 4 | 14 | 4 | 4 | 4 | 4 | 14 | 4 |
| Sym Colour | 1 | 1 | 1 | 1 | 1 | 1 | 1 | 1 | 1 | 1 |
| Rock Type | ELg | ELg | ELbn2 | EL/IB | ELbn2 | ELbn2 | ELbn2 | ELbn2 | EL/IB | ELbn2 |
| SiO ₂ | 60.30 | 53.50 | 62.42 | 54.05 | 58.45 | 57.25 | 55.48 | 52.74 | 54.85 | 55.55 |
| TiO ₂ | 0.34 | 0.37 | 0.85 | 0.85 | 1.20 | 0.94 | 1.01 | 1.21 | 0.70 | 0.92 |
| Al ₂ O ₃ | 15.41 | 16.92 | 17.52 | 18.22 | 16.12 | 18.25 | 18.07 | 18.26 | 18.34 | 19.79 |
| Fe ₂ O ₃ | 4.67 | 5.93 | 6.57 | 8.57 | 10.22 | 8.29 | 8.75 | 11.62 | 10.09 | 8.95 |
| FeO | — | — | — | — | — | — | — | — | — | — |
| MnO | 0.09 | 0.09 | 0.23 | 0.16 | 0.22 | 0.22 | 0.32 | 0.86 | 0.24 | 0.16 |
| MgO | 6.10 | 9.32 | 2.89 | 6.14 | 2.46 | 3.22 | 2.92 | 1.80 | 6.60 | 5.37 |
| CaO | 5.07 | 5.90 | 3.90 | 5.04 | 6.36 | 6.18 | 7.21 | 7.93 | 3.75 | 2.82 |
| Na ₂ O | 7.20 | 3.72 | 1.65 | 5.48 | 3.37 | 2.91 | 4.78 | 2.22 | 3.70 | 4.52 |
| K ₂ O | 0.23 | 1.83 | 3.84 | 0.35 | 1.40 | 2.59 | 1.30 | 3.13 | 1.58 | 1.78 |
| P ₂ O ₅ | 0.09 | 0.09 | 0.13 | 0.15 | 0.19 | 0.15 | 0.15 | 0.23 | 0.16 | 0.14 |
| Total | 100.00 | 99.96 | 100.00 | 100.01 | 99.99 | 100.00 | 99.99 | 100.00 | 100.01 | 100.00 |
| Mg # | 72.12 | 75.68 | 46.56 | 58.66 | 32.28 | 43.48 | 39.79 | 23.48 | 56.44 | 54.30 |
| Cr | 124 | 408 | 116 | 44 | 12 | 40 | 23 | 72 | 51 | 159 |
| Ni | 54 | 180 | 57 | 32 | 7 | 26 | 25 | 50 | 43 | 79 |
| V | 113 | 106 | 192 | 259 | 308 | 204 | 264 | 265 | 248 | 223 |
| Cu | 3 | 2 | 86 | 151 | 42 | 48 | 29 | 77 | 75 | 53 |
| Pb | 3 | 4 | 62 | 4 | 26 | 24 | 4 | 7 | 7 | 69 |
| Zn | 17 | 20 | 432 | 90 | 327 | 222 | 302 | 855 | 175 | 812 |
| K | 1909 | 15191 | 31876 | 2905 | 11621 | 21500 | 10791 | 25982 | 13116 | 14776 |
| Rb | 6 | 53 | 148 | 5 | 44 | 95 | 57 | 122 | 56 | 74 |
| Sr | 167 | 194 | 46 | 114 | 367 | 95 | 144 | 84 | 94 | 184 |
| Nb | 3.6 | 3.6 | 6.4 | 2.6 | 8.7 | 6.7 | 4.9 | 5.7 | 3.0 | 7.5 |
| Zr | 60 | 70 | 120 | 66 | 153 | 152 | 100 | 129 | 53 | 131 |
| Ti | 2038 | 2218 | 5096 | 5096 | 7194 | 5635 | 6055 | 7294 | 4197 | 5515 |
| Y | 14 | 16 | 19 | 22 | 38 | 30 | 27 | 29 | 18 | 28 |
| Th | 4.00 | 4.00 | 5.00 | 4.00 | 10.00 | 9.00 | 7.00 | 9.00 | 5.00 | 7.00 |
| La | 3.64 | — | 16.60 | — | 21.40 | — | — | 18.40 | — | — |
| Ce | 20.60 | — | 35.20 | — | 48.20 | — | — | 41.30 | — | — |
| Pr | — | — | — | — | — | — | — | — | — | — |
| Nd | 11.30 | — | 19.00 | — | 25.30 | — | — | 23.90 | — | — |
| Sm | 2.43 | — | 3.74 | — | 5.56 | — | — | 4.84 | — | — |
| Eu | 0.61 | — | 0.81 | — | 1.45 | — | — | 1.01 | — | — |
| Gd | — | — | — | — | — | — | — | — | — | — |
| Tb | 0.40 | — | 0.67 | — | 0.94 | — | — | 0.82 | — | — |
| Dy | — | — | — | — | — | — | — | — | — | — |
| Ho | 0.50 | — | 0.74 | — | 1.26 | — | — | 1.05 | — | — |
| Er | — | — | — | — | — | — | — | — | — | — |
| Yb | 1.26 | — | 1.75 | — | 3.34 | — | — | 2.70 | — | — |
| Lu | 0.17 | — | 0.25 | — | 0.52 | — | — | 0.39 | — | — |
| Density | 2.47 | 2.54 | 2.47 | 2.55 | 2.54 | 2.53 | 2.54 | 2.59 | 2.56 | 2.53 |

| Sample | 30980 | 30987 | 31641 | 31666 | 31676 | 31683 | 32170 | 32197 | 32806 | 32823 |
|--------------------------------|---------|---------|---------|---------|---------|---------|---------|---------|---------|---------|
| Northings | 5359750 | 5351089 | 5351285 | 5351524 | 5351476 | 5350962 | 5358535 | 5359595 | 5360032 | 5356200 |
| Easting | 378836 | 374094 | 375328 | 375358 | 375258 | 375126 | 379039 | 378779 | 378770 | 376020 |
| Symbol | 4 | 14 | 7 | 7 | 7 | 8 | 9 | 8 | 14 | 2 |
| Sym Colour | 1 | 1 | 1 | 1 | 1 | 1 | 1 | 1 | 1 | 1 |
| Rock Type | ELbn2 | EL/1b | ELbn3 | ELbn3 | ELbn3 | ELbn3 | ELbn3 | ELbn3 | ELbn3 | Eg |
| SiO ₂ | 55.34 | 52.75 | 56.99 | 51.03 | 54.39 | 48.38 | 71.52 | 50.51 | 54.09 | 41.09 |
| TiO ₂ | 0.96 | 1.31 | 2.13 | 2.57 | 2.63 | 3.62 | 0.37 | 3.84 | 1.09 | 0.18 |
| Al ₂ O ₃ | 20.00 | 13.84 | 11.34 | 13.84 | 14.13 | 15.61 | 12.90 | 15.38 | 19.84 | 17.68 |
| Fe ₂ O ₃ | 9.56 | 11.36 | 16.35 | 17.65 | 12.96 | 15.65 | 7.27 | 16.25 | 11.68 | 5.34 |
| FeO | — | — | — | — | — | — | — | — | — | — |
| MnO | 0.14 | 0.21 | 0.19 | 0.34 | 0.18 | 0.29 | 0.06 | 0.20 | 0.11 | 0.18 |
| MgO | 6.07 | 5.70 | 9.07 | 9.07 | 7.40 | 7.09 | 4.79 | 8.24 | 6.71 | 10.56 |
| MgO | 6.07 | 5.70 | 9.07 | 9.07 | 7.40 | 7.09 | 4.79 | 8.24 | 6.71 | 10.56 |
| CaO | 1.16 | 6.29 | 2.76 | 3.46 | 4.54 | 5.46 | 0.38 | 3.32 | 1.48 | 24.35 |
| CaO | 1.16 | 6.29 | 2.76 | 3.46 | 4.54 | 5.46 | 0.38 | 3.32 | 1.48 | 24.35 |
| Na ₂ O | 4.91 | 5.19 | 0.39 | 0.20 | 3.41 | 2.65 | 0.08 | 3.40 | 3.19 | 0.54 |
| Na ₂ O | 4.91 | 5.19 | 0.39 | 0.20 | 3.41 | 2.65 | 0.08 | 3.40 | 3.19 | 0.54 |
| K ₂ O | 1.23 | 1.17 | 0.49 | 1.71 | 0.02 | 0.72 | 2.47 | 0.31 | 1.57 | 0.03 |
| K ₂ O | 1.23 | 1.17 | 0.49 | 1.71 | 0.02 | 0.72 | 2.47 | 0.31 | 1.57 | 0.03 |
| P ₂ O ₅ | 0.14 | 0.18 | 0.30 | 0.34 | 0.32 | 0.52 | 0.16 | 0.35 | 0.24 | 0.06 |
| P ₂ O ₅ | 0.14 | 0.18 | 0.30 | 0.34 | 0.32 | 0.52 | 0.16 | 0.35 | 0.24 | 0.06 |
| Total | 100.02 | 100.00 | 100.02 | 100.01 | 100.01 | 99.99 | 100.00 | 100.00 | 100.01 | 100.02 |
| Mg # | 55.70 | 49.84 | 52.35 | 50.44 | 53.07 | 47.29 | 56.61 | 43.20 | 55.22 | 79.66 |
| Cr | 176 | 19 | 41 | 49 | 57 | 141 | 638 | 152 | 26 | 699 |
| Ni | 70 | 23 | 32 | 36 | 40 | 47 | 106 | 42 | 32 | 266 |
| V | 242 | 325 | 343 | 402 | 408 | 434 | 170 | 470 | 350 | 131 |
| Cu | 31 | 339 | 44 | 46 | 48 | 14 | 30 | 69 | 8 | 2 |
| Pb | 41 | 26 | 24 | 33 | 19 | 13 | 4 | 9 | 9 | 3 |
| Zn | 213 | 281 | 144 | 92 | 137 | 172 | 72 | 189 | 133 | 35 |
| K | 10210 | 4712 | 4067 | 14195 | 166 | 5977 | 20503 | 2573 | 13033 | 249 |
| Rb | 50 | 35 | 13 | 49 | 1 | 23 | 96 | 24 | 65 | 2 |
| Sr | 121 | 187 | 19 | 27 | 62 | 233 | 11 | 170 | 193 | 2 |
| Nb | 7.4 | 0.8 | 18.7 | 21.8 | 24.3 | 21.5 | 6.2 | 32.4 | 3.6 | 2.6 |
| Zr | 136 | 82 | 134 | 153 | 182 | 264 | 98 | 252 | 68 | 26 |
| Ti | 5753 | 7853 | 12769 | 13407 | 13887 | 21702 | 2218 | 23021 | 6533 | 1079 |
| Y | 22 | 29 | 33 | 37 | 41 | 81 | 9 | 56 | 22 | 9 |
| Ta | 7.00 | 3.00 | 2.00 | 1.00 | 2.00 | 4.00 | 14.00 | 4.00 | 9.00 | 1.00 |
| La | 7.82 | 10.80 | 12.30 | — | — | — | 29.70 | 22.30 | — | 4.53 |
| Ce | 17.40 | 25.60 | 29.00 | — | — | — | 59.00 | 54.40 | — | 10.70 |
| Pr | — | — | — | — | — | — | — | — | — | — |
| Nd | 10.30 | 16.60 | 18.10 | — | — | — | 24.50 | 33.70 | — | 6.19 |
| Sm | 2.61 | 4.22 | 4.63 | — | — | — | 4.18 | 8.89 | — | 1.31 |
| Eu | 0.71 | 1.15 | 1.29 | — | — | — | 1.17 | 2.81 | — | 0.44 |
| Gd | — | — | — | — | — | — | — | — | — | — |
| Tb | 0.54 | 0.74 | 0.79 | — | — | — | 0.25 | 1.50 | — | 0.25 |
| Dy | — | — | — | — | — | — | — | — | — | — |
| Ho | 0.79 | 1.02 | 1.10 | — | — | — | 0.25 | 1.47 | — | 0.25 |
| Er | — | — | — | — | — | — | — | — | — | — |
| Yb | 2.23 | 2.61 | 2.62 | — | — | — | 0.86 | 5.49 | — | 0.71 |
| Lu | 0.73 | 0.37 | — | — | — | — | 0.12 | 0.80 | — | 0.10 |
| Density | 2.53 | 2.60 | 2.67 | 2.71 | 2.63 | 2.71 | 2.44 | 2.68 | 2.58 | 2.76 |

APPENDIX 3.

MAJOR ELEMENT ANALYSES FOR HENTY VALLEY CHERTS AND GREYWACKES.

| Sample | 30175 | 32838 | 32839 | 32841 | 32842 | 32844 | 32845 | 32846 |
|--------------------------------|---------|-----------|---------|---------|---------|--------|-------|--------|
| Northing | 5351200 | 5351300 | 5351290 | 5351260 | 5351250 | HR 3 | HR 3 | HR 3 |
| Easting | 375350 | 375250 | 375290 | 375350 | 375400 | 301.7m | 302m | 322.5m |
| Symbol | 1 | 1 | 1 | 1 | 1 | 1 | 1 | 1 |
| Sym Colour | 1 | 1 | 1 | 1 | 1 | 1 | 1 | 1 |
| Rock Type | chert | hem.silt. | chert | chert | chert | gwk | gwk | gwk |
| SiO ₂ | 93.80 | 65.20 | 87.50 | 76.20 | 96.20 | 60.10 | 56.90 | 56.30 |
| TiO ₂ | 0.12 | 0.79 | 0.33 | 0.57 | 0.08 | 0.72 | 0.82 | 0.86 |
| Al ₂ O ₃ | 2.24 | 15.89 | 5.05 | 10.31 | 1.66 | 13.86 | 15.36 | 15.51 |
| Fe ₂ O ₃ | 0.24 | 1.07 | 0.44 | 0.73 | 0.15 | 1.39 | 1.07 | 1.62 |
| FeO | 1.23 | 5.44 | 2.26 | 3.72 | 0.75 | 7.09 | 5.48 | 8.28 |
| MnO | 0.15 | 0.04 | 0.11 | 0.10 | 0.05 | 0.15 | 0.20 | 0.16 |
| MgO | 0.44 | 2.18 | 0.79 | 1.70 | 0.09 | 6.64 | 10.79 | 7.38 |
| CaO | 0.10 | 0.20 | 0.47 | 0.46 | 0.06 | 1.04 | 0.22 | 0.33 |
| Na ₂ O | 0.14 | 0.77 | 0.29 | 0.63 | 0.02 | 1.50 | 1.22 | 2.53 |
| K ₂ O | 0.46 | 4.57 | 1.08 | 2.12 | 0.54 | 1.78 | 1.08 | 1.74 |
| P ₂ O ₅ | 0.06 | 0.12 | 0.11 | 0.11 | 0.03 | 0.09 | 0.08 | 0.12 |
| Total | 98.98 | 96.26 | 98.44 | 96.66 | 99.63 | 94.36 | 93.22 | 94.83 |
| LOI | 0.53 | 3.15 | 1.43 | 2.58 | 0.61 | 4.72 | 5.71 | 4.17 |
| Mg # | 35.12 | 37.78 | 34.58 | 40.87 | 15.39 | 58.65 | 74.90 | 57.46 |
| K | 3818 | 37936 | 8965 | 17598 | 4483 | 14776 | 8965 | 14444 |
| Ti | 719 | 4736 | 1978 | 3417 | 480 | 4316 | 4916 | 5156 |
| Density | 2.28 | 2.43 | 2.31 | 2.37 | 2.26 | 2.52 | 2.54 | 2.55 |

APPENDIX 4.

CHEMICAL ANALYSES AND STRUCTURAL FORMULAE OF CHROME SPINELS FROM
ULTRAMAFICS (30091), QUARTZ MUSCOVITE SANDSTONE (32153) AND
HEMATITE FACIES GREYWACKE (30989).

Chemical analyses (oxide weight %) and structural formulae of chrome spinels from Henty Fault Wedge ultramafic No 30091

| | R 1 | R 2 | R 2 | R 3 | R 4 | R 4A |
|--------------------------------|--------|--------|--------|--------|---------|--------|
| SiO ₂ | 0.00 | 0.00 | 0.00 | 0.01 | 0.00 | 0.00 |
| TiO ₂ | 0.01 | 0.00 | 0.00 | 0.03 | 0.00 | 0.00 |
| Al ₂ O ₃ | 10.75 | 9.61 | 11.16 | 9.10 | 9.14 | 10.33 |
| Cr ₂ O ₃ | 59.33 | 61.05 | 58.84 | 61.99 | 61.62 | 60.40 |
| Fe ₂ O ₃ | 2.24 | 1.54 | 2.64 | 1.72 | 1.39 | 1.52 |
| MgO | 12.04 | 11.87 | 12.41 | 12.01 | 12.01 | 12.24 |
| MnO | 0.29 | 0.36 | 0.33 | 0.27 | 0.30 | 0.15 |
| FeO | 14.78 | 14.72 | 14.24 | 14.74 | 14.42 | 14.51 |
| NiO | 0.06 | 0.02 | 0.14 | 0.06 | 0.00 | 0.00 |
| ZnO | 0.05 | 0.07 | 0.04 | 0.02 | 0.06 | 0.05 |
| Total | 99.55 | 99.24 | 99.80 | 99.96 | 98.9424 | 99.20 |
| Si | 0.0000 | 0.0000 | 0.0000 | 0.0007 | 0.0000 | 0.0000 |
| Ti | 0.0014 | 0.0000 | 0.0000 | 0.0029 | 0.0000 | 0.0000 |
| Al | 1.6539 | 1.4908 | 1.7064 | 1.4053 | 1.4236 | 1.5948 |
| Cr | 6.1246 | 6.3568 | 6.0358 | 6.4203 | 6.4385 | 6.2555 |
| Fe | 0.2198 | 0.1524 | 0.2574 | 0.1698 | 0.1378 | 0.1497 |
| Mg | 2.3426 | 2.3296 | 2.4005 | 2.346 | 2.3666 | 2.3896 |
| Mn | 0.0321 | 0.0406 | 0.0361 | 0.0303 | 0.0339 | 0.0163 |
| Fe | 1.6138 | 1.6207 | 1.5449 | 1.6144 | 1.5938 | 1.5897 |
| Ni | 0.0067 | 0.0025 | 0.0143 | 0.0064 | 0.0000 | 0.0000 |
| Zn | 0.0045 | 0.0067 | 0.0041 | 0.0024 | 0.0057 | 0.0044 |
| Mg# | 59.24 | 58.97 | 60.84 | 59.23 | 59.75 | 60.05 |
| Cr# | 78.74 | 81.00 | 77.96 | 82.04 | 81.89 | 79.69 |

Chemical analyses (oxide weight %) and structural formulae of chrome spinels from Henty Valley Sequence sandstone No 32153.

| | R 2 | R 2A | R 4 | R 4A |
|--------------------------------|--------|--------|--------|--------|
| SiO ₂ | 0.09 | 0.08 | 0.08 | 0.03 |
| TiO ₂ | 0.04 | 0.01 | 0.06 | 0.02 |
| Al ₂ O ₃ | 3.85 | 3.87 | 6.12 | 6.72 |
| Cr ₂ O ₃ | 67.91 | 66.47 | 61.82 | 64.48 |
| Fe ₂ O ₃ | 2.70 | 3.13 | 4.75 | 3.65 |
| MgO | 14.70 | 12.70 | 12.28 | 15.60 |
| MnO | 0.18 | 0.54 | 0.24 | 0.23 |
| FeO | 9.60 | 12.26 | 13.44 | 8.63 |
| NiO | 0.12 | 0.15 | 0.17 | 0.23 |
| ZnO | 0.01 | 0.03 | 0.02 | 0.01 |
| Total | 99.20 | 99.25 | 98.97 | 99.59 |
| Si | 0.0118 | 0.0112 | 0.0102 | 0.0041 |
| Ti | 0.0035 | 0.0014 | 0.0060 | 0.0021 |
| Al | 0.6012 | 0.6128 | 0.9651 | 1.0266 |
| Cr | 7.1103 | 7.0552 | 6.5368 | 6.6093 |
| Fe | 0.2693 | 0.3162 | 0.4778 | 0.3564 |
| Mg | 2.9012 | 2.5420 | 2.4479 | 3.0146 |
| Mn | 0.0204 | 0.0611 | 0.0266 | 0.0248 |
| Fe | 1.0628 | 1.3759 | 1.5031 | 0.9352 |
| Ni | 0.0123 | 0.0161 | 0.0183 | 0.0238 |
| Zn | 0.0014 | 0.0033 | 0.0019 | 0.0007 |
| Mg# | 73.20 | 64.88 | 61.95 | 76.32 |
| Cr# | 92.20 | 92.01 | 87.13 | 86.56 |

Chemical analyses (oxide weight %) and structural formulae of
chrome spinels from Henty Valley Sequence conglomerate No 30989

| | R 1 | R 4 | R 5 | R 5 | R 6 | R 6 |
|--------------------------------|--------|--------|--------|--------|--------|--------|
| SiO ₂ | 0.09 | 0.02 | 0.03 | 0.03 | 0.05 | 0.06 |
| TiO ₂ | 0.05 | 0.27 | 0.14 | 0.10 | 0.07 | 0.04 |
| Al ₂ O ₃ | 4.21 | 6.28 | 10.00 | 8.21 | 6.86 | 6.87 |
| Cr ₂ O ₃ | 63.43 | 61.98 | 60.15 | 61.34 | 55.28 | 55.77 |
| Fe ₂ O ₃ | 4.42 | 1.65 | 0.66 | 0.92 | 8.47 | 9.21 |
| MgO | 10.90 | 7.54 | 9.64 | 8.73 | 8.81 | 10.51 |
| MnO | 0.28 | 0.56 | 0.68 | 0.86 | 0.65 | 0.25 |
| FeO | 15.21 | 20.50 | 17.92 | 18.70 | 18.36 | 16.23 |
| NiO | 0.06 | 0.07 | 0.02 | 0.04 | 0.10 | 0.14 |
| ZnO | 0.04 | 0.04 | 0.05 | 0.09 | 0.03 | 0.06 |
| Total | 98.68 | 98.91 | 99.29 | 99.03 | 98.68 | 99.15 |
| Si | 0.0119 | 0.0034 | 0.0037 | 0.0043 | 0.0073 | 0.0082 |
| Ti | 0.0046 | 0.0284 | 0.0144 | 0.0105 | 0.0070 | 0.0038 |
| Al | 0.6773 | 1.0215 | 1.5711 | 1.3125 | 1.1090 | 1.0931 |
| Cr | 6.8481 | 6.7671 | 6.3401 | 6.5754 | 5.9981 | 5.9556 |
| Fe | 0.4541 | 0.1716 | 0.0663 | 0.0936 | 0.8750 | 0.9364 |
| Mg | 2.2190 | 1.5527 | 1.9157 | 1.7652 | 1.8021 | 2.1147 |
| Mn | 0.0321 | 0.0651 | 0.0769 | 0.0990 | 0.0749 | 0.0290 |
| Fe | 1.7367 | 2.3672 | 1.9984 | 2.1205 | 2.1068 | 1.8333 |
| Ni | 0.0060 | 0.0073 | 0.0023 | 0.0041 | 0.0113 | 0.0156 |
| Zn | 0.0041 | 0.0038 | 0.0045 | 0.0094 | 0.0030 | 0.0059 |
| Mg# | 56.10 | 39.61 | 48.94 | 45.43 | 46.10 | 53.56 |
| Cr# | 91.00 | 86.88 | 80.14 | 83.36 | 84.40 | 84.49 |